DOI: 10.1002/chem.200800139

π-Face Donor Properties of N-Heterocyclic Carbenes in Grubbs II Complexes

Steffen Leuthäußer,[a] Volker Schmidts,[b] Christina M. Thiele,*[b] and Herbert Plenio*[a]

Abstract: The electron-donating properties of eighteen *N*-heterocyclic carbenes (*N*,*N*′-bis(2,6-dimethylphenyl)imidazol)-2-ylidene and the respective dihydro ligands) with 4,4′-R substituted aryl rings (4,4′-R = NEt_2, OMe, Me, H, SMe, F, Cl, Br, I) in the respective Grubbs II complexes were studied using electrochemical techniques. The nature of the 4-R substituent has a strong influence on the $Ru^{II/III}$ redox potentials ranging between $\Delta E_{1/2} = +0.196$ and $+0.532$ V. Three unsymmetrical Grubbs II complexes with 4-R ≠ 4-R′ were also synthesized. Dynamic NMR spectroscopy revealed the restricted rotation around the (NHC)C–Ru bond ($\Delta G = 89$ kJ mol^{-1} at 333 K) resulting in two atropisomers, respectively, with an isomer ratio close to unity. Each of the isomers, that is the two orientations of the 4-R/4-R′ substituted mesityl ring with respect to the R=CHPh unit, gives rise to different redox potentials (4-R = NEt_2, 4-R′ = Br: $\Delta E_{1/2} = +0.232$ and $+0.451$ V). In the oxidized Grubbs II complex (4-R = NEt_2, H) and in the cathodic isomer the electron rich aryl ring is located above the Ru=CHPh unit. This orientational effect provides clear evidence for strong π–π through-space interactions in the Ru^{III} complexes, assuming that the alternative through-bond transfer of electron density is equally efficient in both isomers.

Keywords: dynamic NMR spectroscopy · metathesis · N-heterocyclic carbenes · redox chemistry · ruthenium

Introduction

The use of *N*-heterocyclic carbenes in catalytically active transition-metal complexes is rapidly growing.[1] In olefin metathesis this class of ligands has convincingly demonstrated its superiority over the classic phosphorus(III)-based ligands.[2–7] The performance of NHC-based metal complexes in other fields of catalysis, such as for example Pd-catalyzed cross-coupling reactions, can also be outstanding.[8–13]

A detailed understanding of the steric and electronic properties of NHC ligands in metal complexes is essential to gain full control over the catalytic properties of transition metals[14,15] and a number of experimental studies have been carried out.[16–28] Notable, is work from Nolan who studied various (NHC)Ni(CO)$_3$ complexes[29] and of Herrmann et al. who recently investigated the donating properties of a large number of different NHC ligands.[30] From these and related studies the overall donation of NHC ligands can be determined experimentally, but the decomposition into different factors and their individual contribution is more difficult. The traditional view of NHC ligands being predominantly σ-donors[25,30] was refined and extended to NHC ligands acting as π-donors in electron-deficient metal complexes.[31] Recently, evidence is accumulating that NHC ligands can be regarded as π-acceptors;[32–37] the extent to which this happens is under debate.[34]

However, in certain metal complexes the donating/accepting properties of NHC ligands may not to be limited to effects via the carbene carbon. A structural peculiarity of Grubbs II complexes is the near coplanarity of the Ru=CHAr unit and the *N*-aryl ring belonging to the *N*-heterocyclic carbene ligand. Fürstner et al. were the first to relate the short carbon–carbon distance reported in the crystal structure (around 300 pm for the respective α-carbon atoms) to possible π-stacking interactions between the benzylidene unit and the *N*-aryl rings of the NHC ligand.[38] Short distances between the aryl rings were observed in several solid-state structures of Grubbs II complexes.[39–42]

[a] Dr. S. Leuthäußer, Prof. Dr. H. Plenio
Anorganische Chemie im Zintl-Institut, TU Darmstadt
Petersenstr. 18, 64287 Darmstadt (Germany)
E-mail: plenio@tu-darmstadt.de

[b] V. Schmidts, Dr. C. M. Thiele
Clemens-Schöpf-Institut für Organische Chemie und Biochemie
TU Darmstadt, Petersenstr. 22, 64287 Darmstadt (Germany)
E-mail: cmt@punk.oc.chemie.tu-darmstadt.de

Supporting information for this article is available on the WWW under http://www.chemeurj.org/ or from the author: ^{1}H, ^{13}C NMR assignment of **6a**, **6m-1**, **6m-2** and signal intensities of 1D PFGSE NOE spectra of **6a** and color versions of Figures 1–3 and 6–8.

In a preliminary study we have determined the redox potentials of several Grubbs-type complexes with various substituents at the 4-position of the mesityl flaps.[43] Demonceau et al. demonstrated with different Ru^{II} complexes for ROMP and Kharasch reactions, the use of electrochemical studies to rationalize the catalytic behavior.[44,45] In our experiments we observed a strong influence of the electronic nature of the 4-substituent on the $Ru^{II/III}$ redox potentials. This was unexpected, since seven bonds separate the 4-R substituent from the redox-active Ru center and since the through bond electronic communication is hampered by the orthogonality of the five- and six-membered ring systems (as concluded from solid-state structures). This was seen as evidence for π–π interactions[46] between an aromatic ring at the NHC ligand and the Ru–benzylidene unit. In the meantime, it was shown that even in Grubbs II-type complexes with mixed aryl, alkyl–NHC[40,47–50] or related ligands[49] the aryl groups are located above the benzylidene unit and the alkyl group above the empty coordination site. For bulky alkyl groups steric arguments account for the observed orientation of the *N*-substituents.[42] However, Ledoux et al. have shown that even in methyl, aryl-substituted NHC ligands, the cofacial orientation of *N*-aryl and the Ru–benzylidene group is the preferred one.[47] Grubbs et al. recently reported a Grubbs II-type complex with an aryl, aryl′–NHC ligand displaying a preferential orientation of the more electron-rich aryl above the Ru=CHR group.[51]

Based on detailed electrochemical studies of symmetrical and unsymmetrical Grubbs II-type complexes and extensive NMR studies, we now want to describe in more detail experiments related to the question of whether π–π interactions are of significance in Grubbs II complexes and whether such interactions influence the electron density at the Ru center and the catalytic properties.

Results and Discussion

Synthesis of imidazolium and imidazolinium salts and of the respective saturated and unsaturated Grubbs II complexes: In order to systematically cover a large range of electronic effects in Grubbs II complexes, several symmetrical imidazolium and imidazolinium salts with variable 4-R substituents were synthesized (4-R = OMe, SMe, F, Cl, I) (Scheme 1); others with (4-R = NEt_2, Br, H, Me, $S(O)_2$tolyl) were available from our previous work.[16]

Since this study was undertaken to elucidate potential π–π interactions between the aryl rings and the Ru=CHPh unit, we were also interested in unsymmetrical imidazolinium salts, which originate from two different anilines. Several useful synthetic approaches for the synthesis of such compounds have been reported in the literature.[51–57] Typically, in a stepwise manner an unsymmetrical oxalyl diamide is converted into the respective diamine under strongly reducing conditions using BH_3 or $LiAlH_4$, followed by ring closure. This approach is not compatible with substituents sensitive towards reduction. In order to avoid the use of reductants, we have developed a different route (Scheme 2). Starting from the *N*-β-hydroxyethyl substituted 2,6-dimethylanilines,[58] treatment with HI or Ph_3P/I_2 generated the respective *N*-β-iodoethyl anilinium salt, followed by nucleophilic substitution of the iodide with 2,6-dimethylanilines (4-R = Br or NEt_2). This synthesis can be easily upscaled yielding dekagrams of the corresponding unsymmetrical diamines in good yields (50–70%). The diamines then undergo cyclisation to the respective imidazolinium salts with $HC(OEt)_3$. The respective symmetrical and unsymmetrical Grubbs II-type complexes were obtained from Grubbs I complex and the respective carbene following standard procedures (Scheme 3).[59] This synthesis works for all NHC ligands with the exception of those with strongly electron-withdrawing substituents. Upon exposure of the

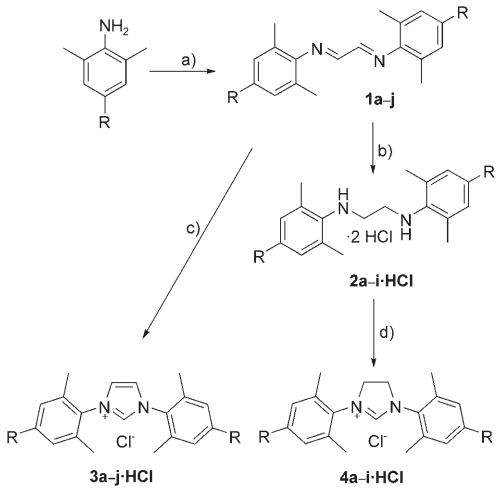

Scheme 1. Synthesis of the imidazolium and imidazolinium salts (**3a, 4a**: 4-R = NEt_2, **3b, 4b**: 4-R = OMe, **3b, 4c**: 4-R = Me, **3d, 4d**: 4-R = H, **3e, 4e**: 4-R = SMe, **3f, 4f**: 4-R = F, **3g, 4g**: 4-R = Cl, **3h, 4h**: 4-R = Br, **3i, 4i**: 4-R = I). a) Ethanol, glyoxal, HCOOH, RT; b) THF, $LiAlH_4$, RT, HCl/H_2O; c) THF, $(CH_2O)_n$, HCl/dioxane, RT; d) $HC(OEt)_3$, HCOOH, 120 °C.

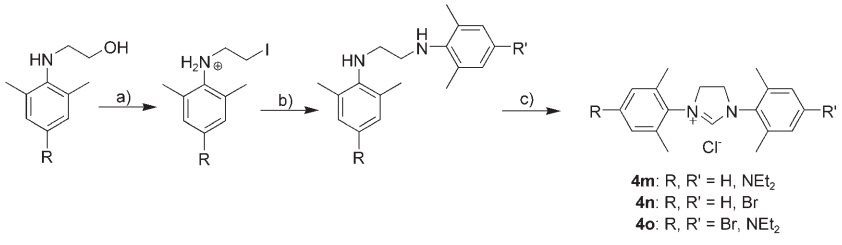

Scheme 2. Synthesis of unsymmetrical imidazolium and imidazolinium salts. a) Neat, 65% aq. HI or I_2/PPh_3; b) DMF, $NaHCO_3$, 4-R-aniline (4-R, 4-R′ = Br, NEt_2), 50 °C, 50–70% yield; c) $HC(OEt)_3$, HCOOH, 120 °C, NH_4Cl.

Grubbs I complex to the 4-S(O_2)tolyl substituted carbene (or the respective Ag^+–NHC complex) no reaction took place. We attribute this failure to the relatively poor electron donation of the respective carbene with 4-R = S(O_2)tolyl; which we have recently shown to be comparable to that of PCy_3.[16]

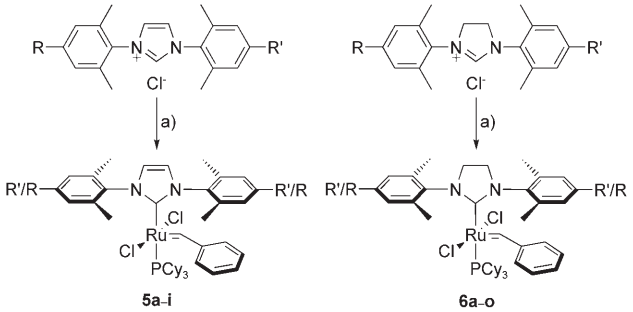

Scheme 3. Synthesis of the 4-R substituted Grubbs II complexes with unsaturated ligands (R = R′ = NEt_2 **5a**, OCH_3 **5b**, Me **5c**, H **5d**, SCH_3 **5e**, F **5f**, Cl **5g**, Br **5h**, I **5i**), with saturated ligands (analogous lettering **6a**, **6b**, **6c**, **6d**, **6e**, **6f**, **6g**, **6h**, **6i**) and R ≠ R′ = NEt_2/H **6m**, Br/H **6n**, NEt_2/Br **6o**. a) Toluene, KO*t*Bu, RT; Grubbs I complex.

Olefin metathesis activity of the 4-R substituted saturated and unsaturated Grubbs II complexes: In order to assess the catalytic activity of olefin-metathesis catalysts in a comparable manner, Grubbs et al. recently suggested a number of diagnostic test reactions.[60] We have applied a few of the newly synthesized complexes in some of these reactions to learn more about the influence of electron density on the olefin-metathesis reactivity.

In the ring-closing metathesis of diethyl diallylmalonate (Figure 1) the activity of the respective Grubbs II catalysts within the two series of complexes with saturated and unsaturated *N*-heterocyclic carbene ligands is ranked according to the electron richness of the respective Ru centres (Grubbs rule):[61,62] 4-NEt_2 > 4-H ⩾ 4-Cl. This order of reactivity was also found in the ring-closing metathesis of diallyltosylamine (Figure 2). In both metathesis reactions the reactivity differences between 4-NEt_2 and 4-H substituted complexes are small compared with what could have been expected from the large differences in the redox potentials. This was unexpected considering the strong donation of the 4-R = NEt_2 group. However, π-stacking interactions can only be operative while the Ru=CHR substructure exists, which is not always the case during the catalytic cycle.

On comparing the catalytic activity of Ru complexes with saturated and unsaturated NHC ligands with identical 4-R group (Figures 1 and 3) the former group is significantly more active, as was previously reported by Grubbs[63] and Fürstner.[38] The activity of the saturated Grubbs II complex with 4-Cl is almost the same as that of the unsaturated Grubbs II complex with 4-NEt_2, while the electron releasing capacity of the unsaturated NHC **4a** (4-R = NEt_2) is significantly higher than that of the saturated NHC **3g** (4-R = Cl)[16] which also translates into very different redox potentials for **5a** and **6g**. Based on the electrochemical experiments (see below) we thus conclude, that the small difference in the electron-releasing capacity of the saturated und unsaturated NHC ligands can hardly account for the much larger differences in the reactivity of the respective saturated and unsaturated Grubbs II complexes.

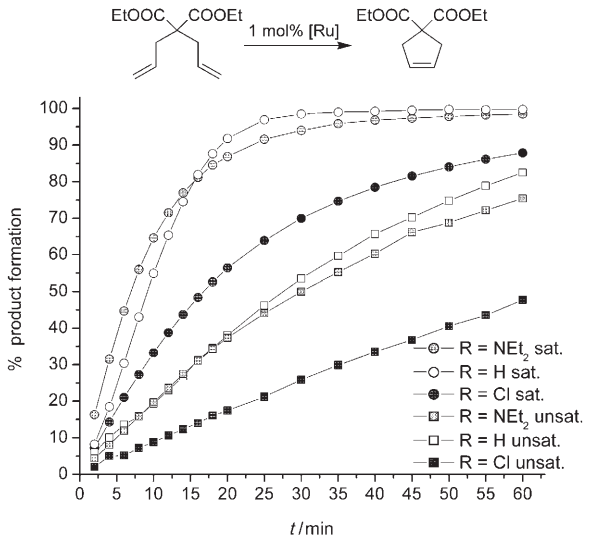

Figure 1. Ring-closing olefin metathesis of diethyl diallylmalonate in CH_2Cl_2 (0.1 M, 1 mol% Grubbs II catalyst, T = 30 °C) (color version available in the Supporting Information).

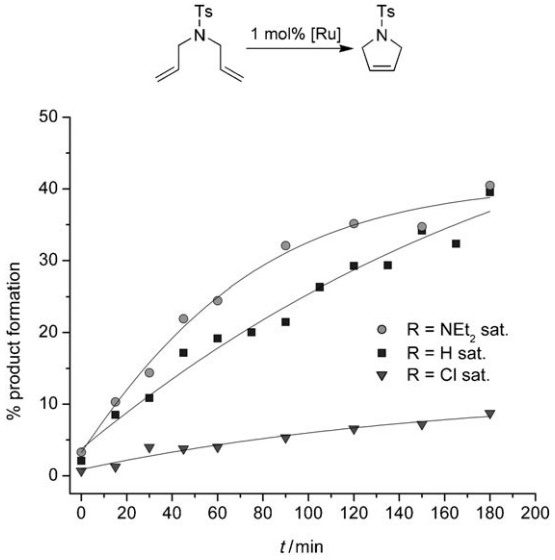

Figure 2. Ring-closing olefin metathesis of diallyltosylamine in CH_2Cl_2 (0.1 M, 1 mol% Grubbs II catalyst **6a**, **d**, **g**, T = 0 °C) (color version available in the Supporting Information).

UV/Vis spectroscopy of Grubbs II complexes: In order to study the influence of the 4-R substituents on the d–d chromophore, UV/Vis spectra of the series of complexes **5** and **6** were recorded (Table 1). All complexes display a typical d–d transition around 500 nm. The use of progressively more

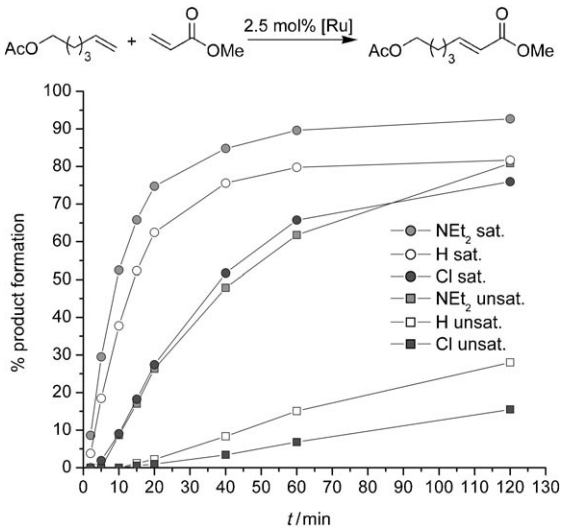

Figure 3. Cross metathesis of hexenylacetate/methacrylate in CH_2Cl_2 (0.4 M, 2.5 mol% Grubbs II catalyst, $T=35$ °C) (color version available in the Supporting Information).

Table 1. UV/Vis data of various Grubbs II complexes (CH_2Cl_2; $c=0.0028$ M.

4-R = 4-R′	Saturated λ_{max} [nm] (ε [L mol^{-1} cm^{-1}])	Unsaturated λ_{max} [nm] (ε[L mol^{-1} cm^{-1}])
4-NEt_2	493 (193)	499 (280)
4-OMe	501 (253)	502 (357)
4-H	502 (169)	504 (146)
4-Cl	501 (221)	503 (273)
4-I	497 (240)	504 (212)

electron-donating substituents in the 4-position has only a small effect on the d–d transitions.

Electrochemical studies

Symmetrical Grubbs II complexes: $Ru^{II/III}$ redox potentials of a large number of Grubbs II complexes **5** and **6** were determined (Table 2) to study how substituents at the aromatic rings influence the electron density at ruthenium. In general, such complexes are characterized by a highly reversible electrochemistry.[43,64] Pronounced differences in the redox potentials between 4-NEt_2 and 4-Br substituted NHC ligands in the saturated ($\Delta E_{1/2}=0.196 \rightarrow 0.538$ V, $\Delta E=344$ mV) and in the unsaturated series ($\Delta E_{1/2}=0.271 \rightarrow 0.532$ V, $\Delta E=261$ mV) of NHC ligands were observed. The much larger effect of the NEt_2 group on the redox potentials of $Ru^{II/III}$ compared to that of the OMe group is based on the much more negative Hammett parameter of the NEt_2 group.[65] The $Ru^{II/III}$ redox potentials of the various Grubbs II complexes are significantly more cathodic than that of the Grubbs I complex ($\Delta E_{1/2}=0.585$ V).[43] This is indicative of a higher electron density at the metal center in the NHC/PCy_3-substituted Grubbs II complexes, than in the PCy_3/PCy_3-substituted Grubbs I species. There appears to be a conflict with results of recent XAS studies by Kennepohl et al., who claims that PCy_3 ligands transfer more electron density on the metal center than an NHC ligand.[66] However, a redox potential denotes the energy difference between two redox states, which is not necessarily correlated with the electron densities of a metal complex in only one oxidation state.

Table 2. Redox potentials of various Grubbs II complexes (CH_2Cl_2/NBu_4PF_6 (0.1 M); internal reference octamethylferrocene ($FcMe_8$); 293 K, scan rate 100 mV s^{-1}).

	Saturated $\Delta E_{1/2}$ [V] (E_a-E_c [mV])	Unsaturated $\Delta E_{1/2}$ [V] (E_a-E_c [mV])
4-R = 4-R′		
6a, 4-NEt_2	0.196 (83)	**5a** 0.271 (80)
6b, 4-OMe	0.454 (74)	**5b** 0.453 (76)
6c, 4-Me	0.455 (76)	**5c** 0.450 (77)
6d, 4-H	0.469 (81)	**5d** 0.470 (85)
6e, 4-SMe	0.479 (76)	**5e** 0.479 (71)
6f, 4-F	0.516 (78)	**5f** 0.514 (82)
6g, 4-Cl	0.529 (78)	**5g** 0.535 (84)
6h, 4-Br	0.538 (82)	**5h** 0.532 (84)
6i, 4-I	0.532 (84)	**5i** 0.528 (82)
4-R ≠ 4-R′		
6m, 4-NEt_2/H	0.219 (102)[a]	0.224[b]
	0.410 (72)[a]	0.420[b]
6n, 4-Br/H	0.503 (85)[a]	0.498[b]
6o, 4-Br/NEt_2	0.226 (104)[a]	0.232[b]
	0.461 (82)[a]	0.451[b]

[a] Cyclic voltammetry. [b] Square wave voltammetry.

The range of the redox potentials in the related (NHC)IrCl(cod) complexes with the same 4-substituents recently studied by us is significantly smaller (saturated NHC: $\Delta E=247$ mV, unsaturated NHC: $\Delta E=214$ mV).[16] Care has to taken when comparing redox potentials of Ir and Ru complexes, nonetheless, the notably stronger influence of the 4-substituents on the redox potential of Grubbs II complexes prompted us to consider additional interactions—other than the normal through-bond component.[67–70] In this respect, interesting transannular interactions between cofacial aromatic ring systems were reported by Gleiter et al. (cofacial cyclobutadienyl–cobalt complexes),[71–73] Boekelheide, Jordan et al. and Speiser et al. (ruthenium-[2.2]paracyclophane)[74,75] to significantly influence cobalt redox potentials.[76]

The redox potentials of Grubbs II complexes with saturated and unsaturated NHC (but identical 4-R groups) are very similar (with the exception of 4-R = NEt_2); indicative of similar donor properties in the two classes of ligands.[77] However, the catalytic properties of the two series of complexes are quite different (see section on Catalysis). We conclude that differences in the catalytic properties of saturated and unsaturated Grubbs II complexes do not originate from dissimilar electron densities at the metal centres. Instead the slightly different steric requirements of saturated and unsaturated NHC ligands (non-planar versus planar five-membered ring) may be responsible.[4,78]

Unsymmetrical Grubbs II complexes: Grubbs II complexes **6m**, **6n** and **6o** with different 4-R, R′ substituents were

shown to exist as pairs of atropisomers by NMR spectroscopy. In one the 4-R substituted aryl flap is located above the Ru–benzylidene unit and the 4-R′ group above the vacant site; in the other one the 4-R′ group is located above the Ru–benzylidene unit and 4-R above the vacant site (Scheme 4). It is an important question whether the unsymmetrical substitution and the different orientations of the 4-R and 4-R′ group have a significant influence on the redox potentials of the respective Grubbs II complexes. Should the two atropisomers persist on the timescale of the electrochemical experiment, two extreme situations are conceivable. In the first scenario, the electron density of the aryl flap, which is modulated by the nature of 4-R and 4-R′ groups, is exclusively transferred to the Ru–benzylidene unit via transannular interactions; then the two different atropisomers must be characterized by significantly different redox potentials. In the second scenario, the electron density of the 4-R group is transferred solely via bonds to the Ru atom. It follows then, that the redox potentials of the two atropisomers have to be identical; as the relative orientation of the 4-R or 4-R′ substituted aryl flaps with respect to the Ru–benzylidene unit should not influence the through-bond transfer. In reality, a mixed situation is likely and it remains to be shown experimentally, whether the two isomers are characterized by sufficiently different redox potentials.

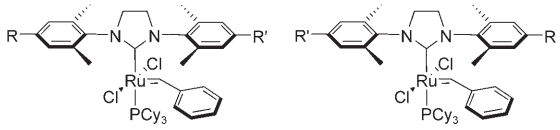

Scheme 4. Atropisomerism in unsymmetrically 4-substituted Grubbs II complexes.

In order to observe two reversible redox waves, the rotation of the NHC ligand around the Ru–C(NHC) should be slow on the timescale of the electrochemical experiment. Based on variable temperature NMR experiments (see section on NMR) the rates of the Ru–C(NHC) rotation in the Grubbs II complexes are known, while the relevant rates of the corresponding process in the paramagnetic Ru^{III} species could not be studied.

Based on an estimate of Ru^{II} dynamic process our initial electrochemical experiments (cyclic voltammetry and square-wave voltammetry) were carried out at temperatures of −20 °C applying scan rates of between 50–1000 mV s^{-1}. In all of these initial experiments using **6m** (4-R = H, NEt_2) two distinct and reversible redox waves were observed. This two wave situation persists even when carrying out the experiments at ambient temperature. It is very important to note here, that we never observed two distinct redox events in any of the symmetrically substituted Grubbs II complexes.

The two redox potentials for the atropisomers of **6m** (Table 2, Figure 4) were determined as $\Delta E_{1/2} = 0.219$ V (cathodic isomer) and $\Delta E_{1/2} = 0.410$ V (anodic isomer), with a peak separation of 191 mV. The redox potential of the cathodic isomer is close to that of the symmetrically substituted **6a** ($\Delta E_{1/2} = 0.196$ V, 4-R = NEt_2, NEt_2), while the potential of the anodic isomer is close to that of **6d** ($\Delta E_{1/2} = 0.469$ V, 4-R = H, H). We thus conclude that the orientation of the 4-R substituted aryl rings relative to the Ru=CHPh group is very important for the redox behavior of the respective Grubbs II complexes.

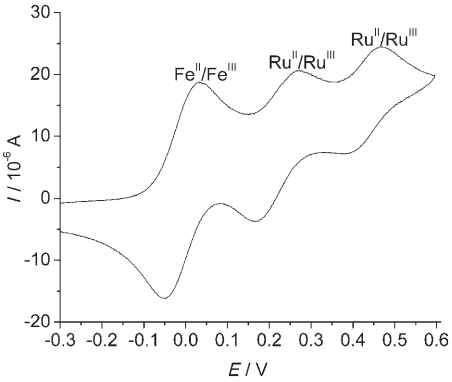

Figure 4. Cyclic voltammogram of **6m** in CH_2Cl_2 $Ru^{II/III}$ 0.219 V (ΔE = 102 mV) and $Ru^{II/III}$ 0.410 V (ΔE = 72 mV) referenced vs. $FcMe_8$ −0.010 V (ΔE = 84 mV).

Electrochemical experiments with **6o** (4-R = Br, NEt_2) again revealed a two wave situation ($\Delta E_{1/2} = 0.226$ and 0.461 V) (Figure 5). As expected, the splitting of the redox potentials is even larger (215 mV). The redox potential of the cathodic isomer of **6o** ($\Delta E_{1/2} = 0.226$ V) is close to that of the cathodic isomer of **6m** ($\Delta E_{1/2} = 0.219$ V). This again demonstrates that the relative orientation of the 4-R groups of the NHC ligand relative to the Ru–benzylidene unit primarily governs the Ru redox potential! In line with this, the redox potentials of the anodic atropisomers of **6m** and **6o** differ significantly (**6m** $\Delta E_{1/2} = 0.410$ V vs. **6o** $\Delta E_{1/2} = 0.461$ V).

With **6n** (4-R = Br, H) only a single redox wave was observed in the cyclic voltammogram and in the square-wave experiment, even though NMR spectroscopy confirms the

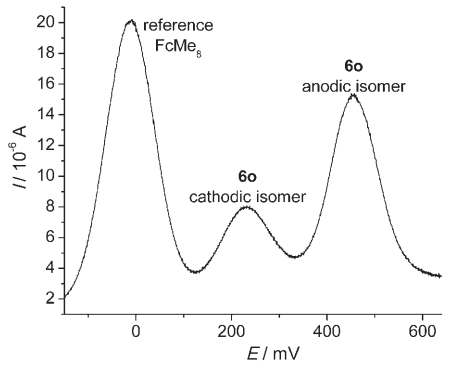

Figure 5. Square-wave voltammogram of **6o** ($FcMe_8$ $\Delta E_{1/2}$ −0.010 V).

existence of two atropisomers. The absence of two redox events for **6n** is not surprising, as the estimated difference of the redox potentials (based on $\Delta E_{1/2}$ of **6d** and **6h**) of the two rotamers should be significantly below 50 mV, which can hardly be resolved using cyclic or square wave voltammetry. The observed $\Delta E_{1/2} = 0.503$ V for **6n** is half way between the redox potentials of **6d** and **6h**.

It could be argued that other events, such as the adventitious protonation of the NEt_2 groups or the coordination of the aniline nitrogen to Ru, lead to two redox events. In order to exclude this, we deliberately added stoichiometric amounts (0.5–2 equivalents) of acid (HBF_4) to **6m** in the electrochemical cell. The presence of acid immediately led to irreversible voltammograms. Nonetheless, we tried to synthesize the respective protonated complex **6m**·H^+. This again turned out to be unsuccessful due to very significant decomposition (^{31}P NMR) of the Grubbs II complexes upon attempted protonation. In order to exclude the potential coordination of the aniline nitrogen we deliberately added *N*,*N*′-diethylaniline to a Grubbs II complex in an electrochemical cell. No change in the CV trace was observed. We thus conclude that the two wave situation is not caused by adventitious protonation of an amino group or its coordination to Ru, but is an intrinsic property of the unsymmetrically substituted Grubbs II complexes.

X-ray crystal structure analysis of 5a (4-R = NEt_2): Within the series of Grubbs II complexes studied here **5a** stands out as the most electron-rich complex and we were interested to learn from the respective crystal structure, whether the rather different electron-donating property of the NHC ligands influences structural parameters of the complex. However, in the solid state the geometric parameters of **5a** (Figure 6) are comparable to those observed in related complexes, as compiled by Fürstner.[38] The Ru–C(NHC) distance of 205.8(4) pm is within the typical range. The carbon–carbon distance between the Ru=C and the N–C(Ph) is fairly short (296.4 pm). The two nitrogen atoms in the 4-position are in a trigonal-planar environment (average CNC angle 119.9°), indicative of efficient nitrogen lone pair donation into the aromatic ring.

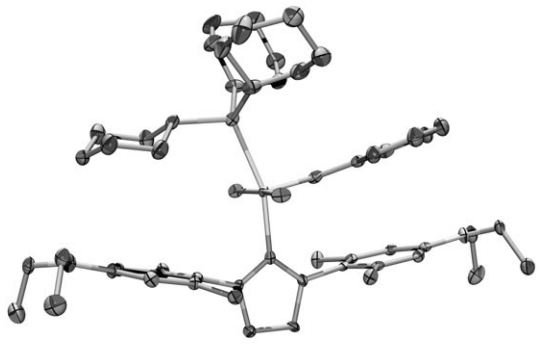

Figure 6. Crystal structure of Grubbs II complex **6a** (4-R = NEt_2) (color version available in the Supporting Information).

NMR Spectroscopy

Symmetrical Grubbs II complexes: We analyzed the various chemical shifts in the ^{1}H, ^{13}C and ^{31}P NMR resonances of the Grubbs II complexes reported here, hoping to observe characteristic changes depending on the electronic nature of the NHC ligands with variable 4-R substituents. However, no such correlations could be found. With the same basic idea, we have determined one bond ^{1}H–^{13}C coupling constants in the carbene unit Ru=*CH*Ph of several complexes. In the complexes studied, the $^1J_{C,H}$ coupling constants are insensitive towards electronic and structural changes: $^1J_{C,H}$ (**6a**; 4-R = NEt_2) = 148.2 Hz (±0.2 Hz) = $^1J_{C,H}$ (**6b**; 4-R = OMe) = 148.2 Hz (±0.2 Hz); $^1J_{C,H}$ (**5b**; 4-R = OMe) = 147.5 Hz (±0.2 Hz) = $^1J_{C,H}$ (**5i**; 4-R = I) not even the replacement of a NHC ligand by a PCy_3 resulting in a Grubbs I complex gave significant changes in the one bond heteronuclear coupling constant ($^1J_{C,H}$ = 147.1 Hz ±0.2 Hz).

Furthermore, we also determined the two bond ^{13}C-^{31}P coupling constants across ruthenium in the (NHC)*C*-Ru-*P*Cy_3 unit of the Grubbs complexes reported here. In the series of saturated Grubbs II complexes the $^2J_{P,C}$ varies between 77–78 Hz, in the unsaturated series complexes between 82-84 Hz. Obviously, there is a significant difference between saturated and unsaturated complexes. The nature of the 4-R substituents does not influence this coupling constant, indicative of a fairly invariant bonding situation in this segment of the complex.

Unsymmetrical Grubbs II complexes: In the NMR spectra of the unsymmetrical complexes **6m**, **6n** and **6o** two different atropisomers are observed, which are characterized by different orientations of 4-R and 4-R′ with respect to the Ru–benzylidene unit (Scheme 4).

Consequently, the two sets of signals for the two isomers can be distinguished. Information about the orientation of the 4-R groups is derived from a complete assignment of both atropisomers at 238 K (see Supporting Information) and the corresponding nuclear Overhauser enhancement (NOE/ROE) between the benzylidene unit and the mesityl flap above it. At that temperature the signals of both mesityl flaps as well as those of the benzylidene unit are completely sharp, whereas at RT virtually all signals are broadened such that a complete assignment is impossible. The assignment of the isomers is aided by the fact that the resonances of this mesityl flap are strongly shielded when located in the anisotropy cone of the benzylidene group. The isomer populations were determined using the respective ^{1}H and ^{31}P integrals. Based on this the following assignment were made: **6m**: 43/57 (major isomer with -NEt_2 group above Ru=CHPh), **6n**: 64/36 (major isomer with -Br above Ru=CHPh), **6o**: 58/42 (major isomer with -Br above Ru=CHPh). The isomer populations are close to unity. Obviously, the energy differences between the isomers are very small (in the range of 1–2 kJ mol^{-1}) not providing evidence in favor of π-stacking interactions.

Dynamic NMR spectroscopy: We have extracted rotational barriers to obtain information on the influence of the 4-R substituents in complexes **6a** and **6m**. The investigation of the symmetrical Grubbs II complex **6a** revealed five important dynamic processes (Scheme 5), denoted with the corresponding rate constants k_0, k_1, k_2, k_3 and k_4. It was noted earlier,[38,51] that the rotation about the Ru–NHC bond (k_4) is restricted in complexes of this kind.

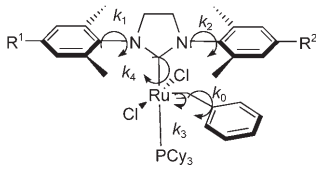

Scheme 5. Dynamic processes in Grubbs II complexes.

All exchange pathways could be nicely followed via 2D exchange spectroscopy (EXSY, Figures 7 and 8). Down to 268 K NOESY spectra, in which signals originating from (the positive) NOE (in the extreme narrowing limit) have different phase with respect to the diagonal, whereas signals due to chemical exchange have the same phase as the diagonal, could be used. When reducing the temperature, however, one easily reaches the intermediate exchange region (zero cross-over of the NOE), where parts of the molecule can exhibit positive NOE signals with other parts showing negative NOE signals. Thus signals due to the negative NOE and due to chemical exchange cannot be distinguished safely. In this motional regime ROESY spectra provide a save way to assign magnetisation transfer pathways. Because of its superior performance we used JS-ROESYs at all temperatures below 268 K.[79] The different exchange pathways are characterized by different symmetry operations.

When determining k_1 and k_2 (rotations of the mesityl flaps) great care has to be taken, as also the rotation of the Ru=CHPh unit (k_3) would lead to an interconversion of the corresponding signals (Me1+Me2 and H1+H2 for k_1 and Me3+Me4 and H3+H4 for k_2). k_3, however, can be monitored by the interconversion of the diastereotopic NHC backbone protons. As long as k_3 cannot be detected (up to 248 K for **6a** and **6m-1**, see Figures 7 and 8) it is safe to determine k_1 and k_2 from the interconversion of the corresponding methyl groups or aromatic protons. One difficulty poses problems for the determination of k_3 and the monitoring of the onset of the corresponding rotational motion: as these protons are geminal diastereotopic protons, they exhibit significant NOE/ROE and their mutual scalar coupling could also lead to TOCSY transfer in the ROE spectrum. The latter is avoided by adjusting the spinlock angle to 45 degrees.[79] The former problem cannot be avoided and leads to the following consequences.

In ROESY experiments ROE and exchange have different signs, such that a signal could still look like a pure ROE, even if some exchange is already contributing (leading to a decrease in signal intensity). So, an ROE-type (different sign of cross peak as compared to diagonal) signal does not automatically mean that there is no exchange (just that ROE is larger as compared to exchange).[95] In NOE experiments, however, at temperatures below the zero cross-over of the NOE (ca. 250 K for the mesityl flaps) NOE and exchange have the same sign. Thus exchange would lead to a positive change in peak intensity. We did not observe any change in signal intensity in 1D PFGSE NOE experiments[80–82] (see below) except that due to temperature dependence of the NOE up to 248 K (see Figure S4, Supporting Information). Above 248 K k_3 starts being observable and k_1 and k_2 cannot be determined reliably anymore. Consequently, we restrict our interpretation of these data to temperatures up to 238 K for k_1 and k_2.

To monitor/determine k_4 we used the signals of the diastereotopic NEt_2 group as the only symmetry operation interconverting the signals is the rotation around the Ru–NHC bond (see Figure 8, no exchange observed at 248 K, crosspeaks appear at 333 K).

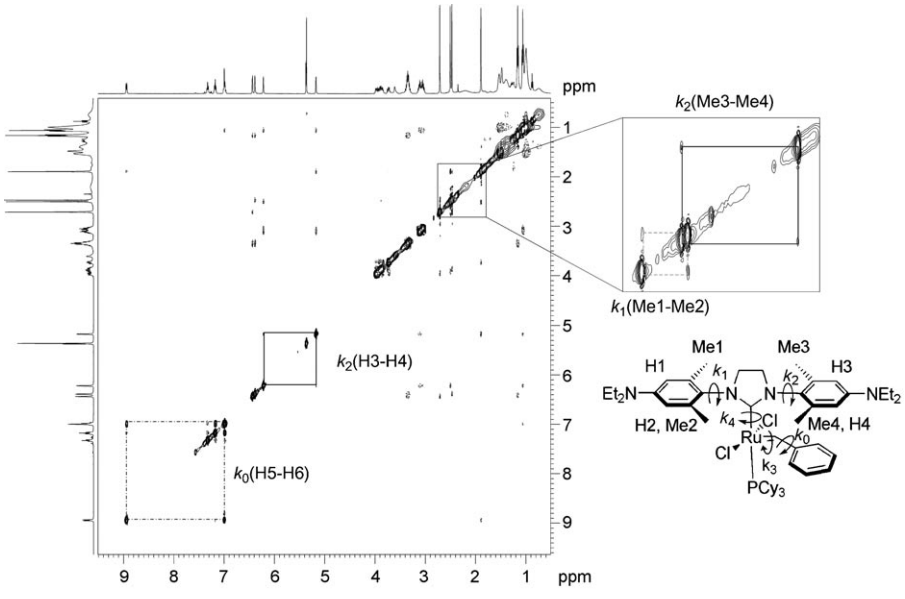

Figure 7. EXSY/JS-ROESY of **6a** at 238 K (200 ms mixing time) and expansion of the region 1.8–3 ppm. Solid, black signals are either diagonal signals or cross peaks indicating chemical exchange, dotted signals show ROE. The different rotational barriers observable at that temperature are indicated by boxes connecting the two diagonal signals with the two cross peaks: Solid black line (see also expansion) for process with corresponding rate constant k_2, dashed line for k_1 and dashed dotted line for k_0 (color version available in the Supporting Information).

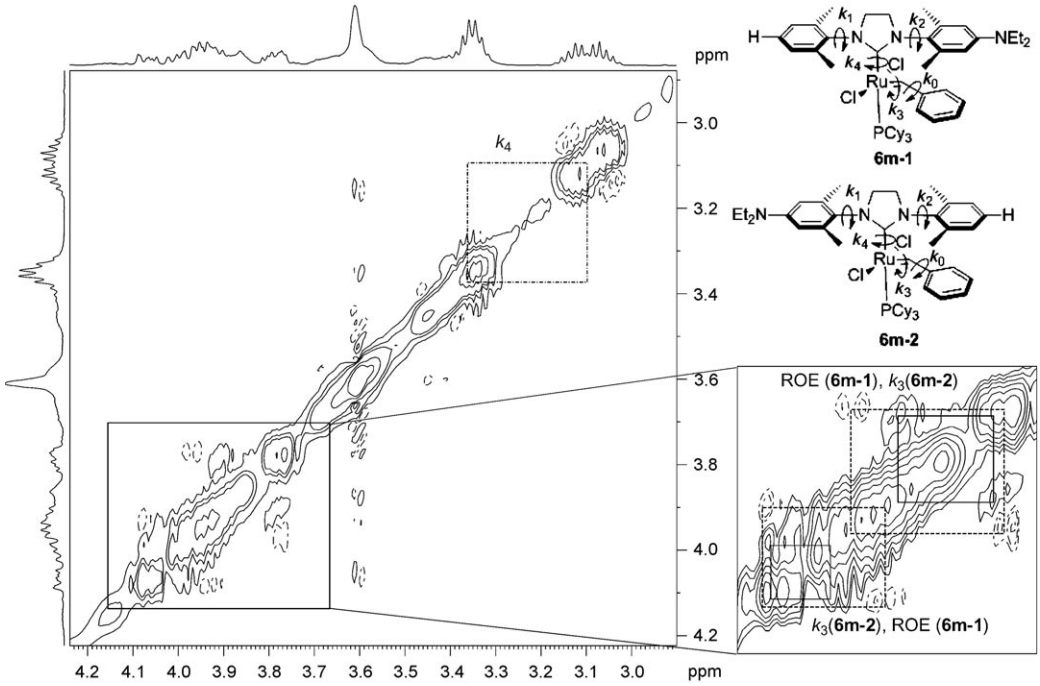

Figure 8. EXSY/JS-ROESY of **6m** at 248 K (200 ms mixing time) and expansion of the region 3.7–4.2 ppm. Solid, black signals are either diagonal signals or cross peaks indicating chemical exchange, dotted signals show ROE. The only rotational process observable at that temperature, k_3 for **6m-2**, is indicated by boxes (solid black lines) connecting the two diagonal signals with the two cross peaks. For **6m-1** this rotational process is not observed at 248 K. Dashed lines show the ROE signals between the respective NHC-backbone signals at 248 K (ROE $\gg$ exchange, see comments in the text and Figure SI4, supporting informations) and indicate where k_3 starts being observable at temperatures of 258 K and higher (data not shown). The dashed dotted line indicates that k_4 (corresponding to the interconversion of **6m-1** and **6m-2**) is not observed at 258 K and at which position k_4 can be observed at 333 K (color version available in the Supporting Information).

Having examined all exchange pathways qualitatively, we performed quantitative dynamic studies by selective 1D PFGSE NOE experiments at different mixing times and different temperatures using the PANIC approach[83,84] for quantification (see Supporting Information).

The fastest rotation occurs about the C–Ph bond in the Ru–benzylidene unit with the corresponding rate constant k_0. We can estimate this barrier, since at the lowest accessible temperature for NMR experiments (193 K) the interchange is almost locked on the NMR timescale, corresponding to a barrier of circa $\Delta G = 52\ kJ\,mol^{-1}$. k_4 describes the slowest process with $\Delta G = 89.2\ kJ\,mol^{-1}$ ($k_4 = 0.1\ s^{-1}$ at 333 K for **6a**, $k_4 = 0.2\ s^{-1}$ at 333 K for unsymmetrical **6m**), which is different from the corresponding barrier in related fluorine-substituted Grubbs complexes (75 $kJ\,mol^{-1}$), but comparable that in the Grubbs II complex (91 $kJ\,mol^{-1}$).[51] The unsymmetrical Grubbs II complexes such as **6m**, **6n** and **6o** therefore exist as two atropisomers at room temperature,[85] whose interconversion is very slow on the NMR timescale. It is, however, fast enough to preclude the purification of the two atropisomeric complexes by conventional techniques.

As reported earlier ^1H signals of the aromatic proton of the mesityl ring above the benzylidene unit (denoted H3 and H4) are extensively broadened in spectra recorded at room temperature; whereas ^1H signals of the aromatic protons of the mesityl ring above the empty coordination site (H1 and H2) are isochronous and rather sharp at room temperature. This has been interpreted to be due to two different rotational barriers ($k_1 \neq k_2$, k_1 fast at RT, k_2 slow at RT) and indicative of π-stacking, for which additional evidence was provided by comparing reactivity and ^1H spectra in chloroform and benzene.[38]

On closer examination of the spectra of complexes **6a** and **6m**, (especially after being able to assign all resonances, see Experimental Section and Supporting Information), we realized that H1 and H2 are accidentally isochronous (the corresponding methyl groups Me1 and Me2, however, are still anisochronous). We were able to extract rate constants for k_1 and k_2 at four temperatures (223–238 K). At all temperatures k_1 equals k_2 ($k_1 = k_2$) within experimental error (see Table 3) as determined from the signals of the methyl groups (Me1+Me2 and Me3+Me4, respectively). For the mesityl flap above the benzylidene unit we were even able to check for consistency by using H3 and H4. From these temperature dependent measurements of the rate constants we had access to $\Delta G^{\neq}$, $\Delta H^{\neq}$ and $\Delta S^{\neq}$. The latter two, however, are notoriously error prone, so that comparisons have to be viewed with caution.

When comparing the complexes **6a** and **6m-1** (NEt_2 above benzylidene moiety) only minute differences are observed; for **6m-2** (H above the benzylidene moiety), however, the rotation of the Ru=CHPh group (k_3) sets in much earlier. Whether this trend is observable also in other com-

Table 3. Rate constants for the different rotations in complex **6a** and **6m** (two atropisomers, 4-R = NEt_2, 4-R′ = H, **6m-1**, 4-R above benzylidene unit, **6m-2**; 4-R′ above benzylidene unit) and corresponding ΔG^{+}, ΔH^{+} and ΔS^{+}. The latter two determined from measurements at temperatures 223 to 238 K (as at temperatures above 248 K a small contribution of k_3 is observed additionally to k_1/k_2; see main text and Figure SI4). For **6m-1** comparable values are obtained, for **6m-2**, however, the rotational process corresponding to k_3 sets in much earlier.

Complex	T [K]	Rate constant	k_x [s^{-1}]	ΔG^{+} [kJ mol^{-1}]	ΔH^{+} [kJ mol^{-1}]	ΔS^{+} [J mol^{-1}]
	223	k_1	0.005	64.0 (±0.1)	61.6 (±2)	−11.1 (±9)
	228	k_1	0.009	64.2 (±0.2)		
	233	k_1	0.021	64.1 (±0.1)		
	238	k_1	0.040	64.2 (±0.1)		
	248	k_1	0.27	63.0 (±0.1)		
	258	$k_1 + k_3$	0.92	63.0 (±0.1)		
	268	$k_1 + k_3$	3.09	62.9 (±0.3)		
6a						
	223	k_2	0.005	63.8 (±0.2)	61.4 (±4)	−10.8 (±15)
	228	k_2	0.010	64.1 (±0.2)		
	233	k_2	0.023	63.9 (±0.1)		
	238	k_2	0.044	64.0 (±0.1)		
	248	k_2	0.24	63.3 (±0.1)		
	258	$k_2 + k_3$	1.08	62.7 (±0.1)		
	268	$k_2 + k_3$	2.51	63.3 (±0.3)		
	333	k_4	0.10	89.3 (±0.2)	n.d.	n.d.
	238	k_1	0.10	62.4 (±0.1)	n.d.	n.d.
6m-1	238	k_2	0.10	62.4 (±0.1)	n.d.	n.d.
	333	k_4	0.20	87.1 (±0.2)	n.d.	n.d.
	238	$k_1 + k_3$	0.22	60.9 (±0.1)	n.d.	n.d.
6m-2	238	$k_2 + k_3$	0.24	60.7 (±0.1)	n.d.	n.d.
	333	k_4	0.20	87.1 (±0.2)	n.d.	n.d.

plexes and can be related to the properties of these Grubbs II complexes will be investigated in the future.

Orientation of the 4-R substituted mesityl versus the Ru–benzylidene unit: The electrochemical experiments show that the orientation of the 4-R group relative to the Ru–benzylidene unit exerts a strong influence on the Ru redox potentials. A very important question is which redox potential (cathodic and anodic isomer) corresponds to which orientation of the 4-R substituted aryl group. However, the integration of ^{1}H and ^{31}P spectra of **6m**, **6n** and **6o** revealed that the energy differences between the two orientations are in the 1–2 kJ mol^{-1} range. With a view to the very small energy differences between the respective atropisomers, the integration of the square-wave voltammograms is not suitable to resolve the question of which orientation of the 4-R group gives rise to which redox potential. The same argument applies to the use of X-ray crystal structure analysis.

We have therefore taken a different approach. The isomeric mixture of **6m** was chemically oxidized using $Fc^{+}PF_6^{-}$.[86] This process leads to the selective oxidation of the cathodic isomer. NHC ligands are known to also stabilize metals in higher oxidation states.[87] When the reaction is carried out under conditions which allow the equilibration of the two Ru^{II} atropisomers, the isomer mixture is converted almost quantitatively into the cathodic isomer.[88] The presence of only a single oxidized isomer was verified by reductive cyclic voltammetry. Attempts to resolve the NMR spectrum of the paramagnetic species were unsuccessful due to extreme line broadening and/or decomposition of the Ru^{III} species. Following the oxidation of the Grubbs II complex the reduction was effected using $FcMe_8$ (octamethylferrocene) at temperatures low enough to preclude the equilibration of the isomers. This reaction proceeds to completion within 30 min at −78 °C (TLC control). For the following work-up it is mandatory to keep the temperature always below −30 °C to slow down isomerization. Simple filtration of the reaction mixture over silica sufficed to remove the paramagnetic impurities. Evaporation of the solvents (CH_2Cl_2, Et_2O) was done at −78 °C. Following this simple procedure the enriched cathodic isomer (anodic/cathodic 15:85, compared with 43:57 at RT equilibrium) was isolated. This experiment also establishes the full reversibility of the cyclic voltammograms. Following the full RT isomerisation, the initial 43:57 ratio of the atropisomers of **6m** was detected. The ^{1}H and ^{31}P NMR spectra of the 85% component allow the assignment of the enriched isomer as the one with the 4-R = NEt_2 located above the Ru=CHPh group. This provides strong support for the π-π interaction between the two aryl groups. The electrochemical data demonstrate that the electronic density at the Ru is primarily modulated by the nature of the 4-R group located above the Ru–benzylidene group; the influence of the 4-R group above the empty coordination site seems to be much weaker; effectively being limited to the much weaker through bond component.

Summary and Conclusions

We studied the catalytic, electrochemical, dynamic and structural properties of several Grubbs II complexes, in which the nature of the substituents in the 4-position of the mesityl flaps of the NHC ligand was varied systematically. From these experiments we can draw a number of conclusions:

a) The differences in the reactivity of Grubbs II complexes with saturated and unsaturated NHC ligands do not originate from different electron density at the Ru center. The redox potentials of the various Grubbs II complexes

confirm that the electron donation of saturated and unsaturated NHC ligands is similar. Nonetheless, saturated complexes Grubbs II complexes are initially more active in olefin metathesis than the unsaturated ones; subtle steric effects could play a decisive role.

b) The nature of the 4,4′-substituents on the mesityl flaps of the NHC ligands has a significant influence on the electron density at Ru and on the catalytic properties of Grubbs II complexes; a range of 336 mV is covered between the most and the least electron donating substituents attached to the mesityl flaps.

c) The use of unsymmetrically substituted NHC ligands (bearing different 4,4′-substituents on the mesityl rings) in Grubbs II complexes results in two atropisomers, which are characterized by different orientations of the 4 and 4′-substituents relative to the Ru–benzylidene unit and more importantly also by different redox potentials. More specifically we learnt that the mesityl flap located above the Ru=CHPh unit is primary responsible for the redox potentials. This observation is not compatible with an exclusive through-bond electron transfer of the electron density from the 4-substituents to Ru, but matches well with considerable transannular interactions of the mesityl flap and the Ru=CHR unit. The fact that the ratio of the different atropisomers is close to unity, indicates that the effect of π-stacking on isomer ratio is weak in the Ru^{II} complexes, while it appears to be much stronger in the oxidized Grubbs II complexes.

The work described here provides firm evidence for *N*-aryl-substituted NHC ligands acting as π-face donors in the oxidized Grubbs II complexes. This quality will be of relevance for other NHC metal complexes.

Experimental Section

General experimental methods: All chemicals were purchased as reagent grade from commercial suppliers and used without further purification, unless otherwise noted. THF was distilled over potassium and benzophenone under argon. ^{1}H, ^{13}C and ^{31}P NMR spectra were recorded on Bruker DRX 500 at 500.15, 125.75 and 202.46 MHz, respectively, or on Bruker DRX 300 at 300 or 75.07 MHz. The chemical shifts are given in parts per million (ppm) on the delta scale (δ) and are referenced to tetramethylsilane (^{1}H, ^{13}C NMR = 0 ppm), ^{31}P NMR (65% aq. H_3PO_4 = 0 ppm), Abbreviations for NMR data: s = singlet; d = doublet; t = triplet; q = quartet; m = multiplet; brs = broad signal; arom. = aromatic protons.

$^1J_{C,H}$ coupling constants were measured using ω_2 coupled HSQC spectra (with a digital resolution of 0.2 Hz), $^2J_{C,P}$ from the ^{13}C spectrum. All variable temperature NMR experiments were performed with a TBI probe with selective ^{31}P coil, which was also used for ^{31}P decoupling, equipped with a BTO-2000 (temperature reference stabilizing unit, no temperature correction necessary). Assignment at low temperature was performed using ^{1}H, ^{13}C, HSQC (^{31}P decoupled, using adiabatic pulses for inversion and refocusing pulses on ^{13}C), HMBC and JS-ROESY spectra, which are (with exception of JS-ROESY) available in the Bruker pulse sequence library. JS-ROESY[79] was implemented and recorded with typical mixing times of 200 to 600 ms and relaxation delays of typically 1 s for qualitative exchange/NOE mapping.

For quantitative determination of rate constants from transient 1D NOE experiments, first T_1 times were determined using the inversion-recovery method. The relaxation delays in the 1D PFGSE NOE experiments[82] were set accordingly (10 s). A 20 ms Gaussian pulse was chosen for selective irradiation in most cases. For each rate constant (at each temperature) five NOE experiments were performed with mixing times between 100 and 600 ms. The integral ratio of exchange peak to irradiated peak was used (PANIC approach[83,84]) for quantification. Only those values within the initial rate approximation were used for the fit of peak volume versus mixing time (up to 400 ms in most cases) leading directly to the rate constant as slope of the corresponding plot.[89] ΔG^{+}, ΔH^{+} and ΔS^{+} were obtained using the Eyring equation.[90]

GC analysis were performed on CP-Sil 8 CB column (15 m, d_i = 0.25 mm, Varian) with Perkin Elmer Clarus 500 GC AutoSystem. Electrochemistry: The standard electrochemical instrumentation consisted of an EG&G 273 A-2 potentiostat galvanostat. A three-electrode configuration was employed. The working electrode was a Pt disk (diameter 1 mm) sealed in soft glass with a Pt wire as counter electrode. The pseudo reference electrode was an Ag wire. Potentials were calibrated internally against the formal potential of octamethylferrocene (−0.010 V vs Ag/AgCl). All cyclic voltammograms and square wave voltammograms were recorded in dry CH_2Cl_2 under an atmosphere of Ar. As supporting electrolyte NBu_4PF_6 (c = 0.1 mol L^{-1}) was used. Square wave voltammetry (pulse height 50 mV; frequency 15 Hz). Thin layer chromatography (TLC) was performed using silica gel 60 F 254 (0.2 mm) on aluminium plates. For preparative chromatography E. Merck silica gel 60 (0.063–0.20 mesh) was used.

The following compounds were prepared according to literature procedures: 2,6-dimethyl-4-iodoaniline,[91] as described for the 2,6-diisopropyl derivative, 2,6-dimethyl-4-fluoroaniline,[92] 2,6-dimethyl-4-(methylthio)aniline,[93] *N*,*N*′-bis(2,4,6-trimethylphenyl)imidazolium chloride and *N*,*N*′-bis(2,4,6-trimethylphenyl)imidazolinium chloride,[94] *N*,*N*′-bis(2,6-dimethylphenyl)imidazolium chloride and *N*,*N*′-bis(2,6-dimethyl-4-bromophenyl)imidazolium chloride,[16] *N*,*N*′-bis(2,6-dimethyl-4-bromophenyl)imidazolinium chloride,[16] *N*,*N*′-bis(2,6-dimethyl-4-*N*,*N*′-diethylaminophenyl)-imidazolium chloride,[16] *N*,*N*′-bis(2,6-dimethyl-4-*N*,*N*′-diethylaminophenyl)imidazolinium chloride.[16]

Synthesis of the anilines

2,6-Dimethyl-4-fluoroaniline:[92] 3,5-Dimethylaniline (34.5 mL, 268 mmol, 1 equiv) was diazotized at 0 °C using $NaNO_2$ and HCl. The resulting solution of the corresponding diazonium chloride was treated with aq. HBF_4 (8 M, 33.50 mL, 268 mmol, 1 equiv) stirred at 0 °C for 2 h and the diazonium tetrafluoroborate was filtered off. The white solid was washed with cold water (20 mL), a cold mixture of methanol/Et_2O 1:1 (20 mL) and Et_2O (20 mL). The product was dried in vacuo. The diazonium tetrafluoroborate was heated to 75 °C at which point the evolution of N_2 und BF_3 started. After the evolution had ceased the crude product was distilled. 3,5-Dimethylfluorbenzene (14.51 g, 55%) was obtained as a colorless oil. ^{1}H NMR (200 MHz, $CDCl_3$): δ = 2.29 (s, 6H, CH_3), 6.68 ppm (m, 3H, arom.).

To neat 3,5-dimethylfluorobenzene (14.51 g, 117 mmol, 1 equiv) was added dropwise fuming HNO_3 (96%, 4.77 mL, 7.25 g, 1 equiv) at −15 °C. The mixture was stirred for 3 h at room temperature, poured into water (100 mL) and extracted with Et_2O (3 × 100 mL). The combined organic layers were washed with saturated Na_2CO_3 solution and dried over $MgSO_4$. The solvent was evaporated to give a mixture of 2,6-dimethyl-4-fluoronitrobenzene and 2,4-dimethyl-6-fluoronitrobenzene. The two isomers were separated by column chromatography (silica gel, cyclohexane/ethyl acetate 8:1, R_f = 0.40). 2,6-Dimethyl-4-fluoronitrobenzene (3.63 g, 18%) was obtained as a colorless oil. ^{1}H NMR (500 MHz, $CDCl_3$): δ = 2.32 (s, 6H, CH_3), 6.82 ppm (d, $^3J_{H,F}$ = 9 Hz, 2H, arom.); ^{13}C NMR (126 MHz, $CDCl_3$): δ = 17.8, 115.6 (d, $^2J_{C,F}$ = 24 Hz), 132.8 (d, $^3J_{C,F}$ = 9 Hz), 148.7, 162.2 ppm (d, $^1J_{C,F}$ = 252 Hz). 2,6-Dimethyl-4-fluoronitrobenzene (3.63 g, 21.5 mmol, 1 equiv) was dissolved in glacial acetic acid (150 mL) and hydrogenated using palladium on charcoal as catalyst (10 wt% Pd, 2.29 g, 2.2 mmol, $p(H_2)$ = 5 bar). After 5 h the reaction mixture was filtrated over Celite, neutralized with NaOH solution (1 M) and extracted with CH_2Cl_2 (3 × 100 mL). The combined organic layers were

dried over $MgSO_4$ and the solvent was evaporated to yield 2,6-dimethyl-4-fluoroaniline (1.97 g, 66%). ^{1}H NMR (300 MHz, $CDCl_3$): δ = 2.15 (s, 6H, CH_3), 3.39 (brs, 2H, NH_2), 6.66 ppm (d, $^3J_{H,F}$ = 9.0 Hz, 2H, arom.); ^{13}C NMR (75.5 MHz, $CDCl_3$): δ = 17.8, 114.4 (d, $^2J_{C,F}$ = 22.4 Hz), 123.1 (d, $^3J_{C,F}$ = 7.5 Hz), 138.6, 155.6 ppm (d, $^1J_{C,F}$ = 235 Hz).

2,6-Dimethyl-4-methoxyaniline: 2,4-Dinitroaniline (36.62 g, 0.2 mol, 1 equiv) was diazotized using $NaNO_2$ und HCl. The resulting solution of the diazonium chloride was transferred via cannula to a solution of 3,5-dimethylanisole (15.0 g, 110 mmol) in glacial acetic acid (350 mL) at 0°C. The reaction mixture was stirred for 24 h at room temperature and poured into water (1 L). The resulting red azo dye was filtered off and redissolved in $CHCl_3$. The solution was washed with saturated $NaHCO_3$ solution and dried over $MgSO_4$. The solvent was evaporated to yield the crude azo dye (23.97 g).

A sample (10 g, 30.3 mmol, 1 equiv) was dissolved in THF/ethanol 8:1 (150 mL) and hydrogenated using palladium on charcoal as catalyst (10 wt% Pd, 3.22 g, 3.0 mmol, $p(H_2)$ = 5 bar). After 5 h the reaction mixture was filtrated over Celite and the solvent was evaporated. The crude product was purified by column chromatography (silica gel, cyclohexane/ethyl acetate 2:1) to yield 2,6-dimethyl-4-methoxyaniline (0.89 g, 19%). ^{1}H NMR (300 MHz, $CDCl_3$): δ = 2.17 (s, 6H, CH_3), 3.34 (s, 2H, NH_2), 3.73 (s, 3H, OCH_3), 6.55 ppm (s, 2H, arom.); ^{13}C NMR (75.5 MHz, $CDCl_3$): δ = 18.0, 55.7, 113.9, 123.2, 136.4, 152.0 ppm.

General procedure for the synthesis of diimines 1

The corresponding aniline (2 equiv) was dissolved in ethanol (2 mL per mmol), treated with aqueous glyoxal solution (40% weight; 1 equiv) and three drops of formic acid. The reaction mixture was stirred over night. The yellow solid was filtered off, washed with cold MeOH and dried in vacuo. The volume of the mother liquor was halved and the remaining solution kept at 4°C over night for a second batch of product.

***N,N′*-Bis(2,6-dimethyl-4-methoxyphenyl)ethylenediimine (1b)**: 2,6-Dimethyl-4-methoxyaniline (0.89 g, 5.89 mmol, 2 equiv), glyoxal (0.34 mL, 428 mg, 2.95 mmol, 1 equiv). Yield: 708 mg (74%). ^{1}H NMR (300 MHz, $CDCl_3$): δ = 2.20 (s, 12H, CH_3), 3.79 (s, 6H, CH_3), 6.57 (s, 4H, arom.), 8.11 ppm (s, 2H, CH); ^{13}C NMR (75 MHz, $CDCl_3$): δ = 18.5, 55.3, 113.7, 128.6, 143.3, 156.7, 163.5 ppm.

***N,N′*-Bis(2,6-dimethyl-4-thiomethylphenyl)ethylenediimine (1e)**: 2,6-Dimethyl-4-thiomethylaniline (3.0 g, 17.9 mmol, 2 equiv), glyoxal (1.03 mL, 1.30 g, 8.97 mmol, 1 equiv). Yield: 2.44 g (76%). ^{1}H NMR (200 MHz, $CDCl_3$): δ = 2.17 (s, 12H, CH_3), 2.49 (s, 6H, CH_3), 7.02 (s, 4H, arom.), 8.09 ppm (s, 2H, CH); ^{13}C NMR (75 MHz, $CDCl_3$): δ = 16.4, 18.3, 127.0, 127.6, 134.1, 147.5, 163.4 ppm.

***N,N′*-Bis(2,6-dimethyl-4-fluorphenyl)ethylenediimine (1f)**: 2,6-Dimethyl-4-fluoroaniline (6.00 g, 43.1 mmol, 2 equiv), glyoxal (2.5 mL, 21.6 mmol, 1 equiv). Yield: 4.85 g (75%). ^{1}H NMR (300 MHz, $CDCl_3$): δ = 2.18 (s, 12H, CH_3), 6.81 (d, $^3J_{H,F}$ = 9 Hz, 4H, arom.), 8.09 ppm (s, 2H, CH); ^{13}C NMR (75 MHz, $CDCl_3$): δ = 17.4, 113.7 (d, $^2J_{C,F}$ = 22 Hz), 127.7 (d, $^3J_{C,F}$ = 7.5 Hz), 144.4 (d, $^4J_{C,F}$ = 2.3 Hz), 158.7 ($^1J_{C,F}$ = 243 Hz), 162.9 ppm.

***N,N′*-Bis(2,6-dimethyl-4-chlorophenyl)ethylenediimine (1g)**: 2,6-Dimethyl-4-chloroaniline (7.19 g, 46 mmol, 2 equiv), glyoxal (2.63 mL, 23 mmol, 1 equiv). Yield: 4.27 g (56%). ^{1}H NMR (500 MHz, $CDCl_3$): δ = 2.15 (s, 12H, CH_3), 7.08 (s, 4H, arom), 8.07 ppm (s, 2H, CH); ^{13}C NMR (126 MHz, $CDCl_3$): δ = 18.2, 128.3, 128.4, 129.4, 148.2, 163.7 ppm.

***N,N′*-Bis(2,6-dimethyl-4-iodophenyl)ethylenediimine (1i)**: 2,6-Dimethyl-4-iodoaniline (2.87 g, 11.6 mmol, 2 equiv), glyoxal (0.67 mL, 5.81 mmol, 1 equiv). Yield: 2.04 g (68%). ^{1}H NMR (300 MHz, $CDCl_3$): δ = 2.12 (s, 12H, CH_3), 7.43 (s, 4H, arom), 8.05 ppm (s, 2H, CH); ^{13}C NMR (75 MHz, $CDCl_3$): δ = 18.0, 89.2, 129.0, 137.0, 149.6, 163.6 ppm.

General procedure for the synthesis of diamine dihydrochlorides 2

The corresponding ethylenediimine (1 equiv) was placed in a Schlenk flask and dissolved in anhydrous THF (10 mL per mmol) under argon. The solution was cooled to 0°C and $LiAlH_4$ pellets (2 equiv) were added. The reaction mixture was stirred over night at room temperature and poured carefully into an excess of an ice/conc. HCl mixture.

Workup A: The white precipitate was collected by filtration, washed with cold water and dried in vacuo.

Workup B: The reaction mixture was basified using NaOH and extracted with Et_2O (3×250 mL). The combined organic layers were dried over $MgSO_4$ and the solvent was evaporated in vacuo.

***N,N′*-Bis(2,6-dimethyl-4-methoxyphenyl)ethylenediamine dihydrochloride**: *N,N′*-Bis(2,6-dimethyl-4-methoxyphenyl)ethylenediimine (415 mg, 1.28 mmol, 1 equiv); $LiAlH_4$ (97 mg, 2.56 mmol, 2 equiv). *Workup A*: Yield: 310 mg (60%). ^{1}H NMR (300 MHz, [D$_6$]DMSO): δ = 2.43 (s, 12H, $ArCH_3$), 3.54 (s, 4H, NCH_2CH_2N), 3.72 (s, 6H, OMe), 3.0–4.2 (brs, 4H, NH_2), 6.72 ppm (s, 4H, arom.); ^{13}C NMR (75 MHz, [D$_6$]DMSO): δ = 18.3, 46.6, 55.2, 114.6, 133.3 ppm.

***N,N′*-Bis(2,6-dimethyl-4-thiomethylphenyl)ethylenediamine dihydrochloride (2e)**: *N,N′*-Bis(2,6-dimethyl-4-thiomethylphenyl)ethylenediimine (920 mg, 2.58 mmol, 1 equiv); $LiAlH_4$ (196 mg, 5.16 mmol, 2 equiv). *Workup A*: Yield: 944 mg (84%). ^{1}H NMR (300 MHz, [D$_6$]DMSO): δ = 2.44 (s, 6H, SCH_3), 2.45 (s, 12H, $ArCH_3$), 3.63 (s, 4H, CH_2), 7.03 (s, 4H, arom.), 6.0–8.5 ppm (brs, 4H, NH_2); ^{13}C NMR (75 MHz, [D$_6$]DMSO): δ = 14.7, 18.2, 46.2, 126.7, 132.4, 133.3, 137.0 ppm.

***N,N′*-Bis(2,6-dimethyl-4-fluorophenyl)ethylenediamine dihydrochloride (2f)**: *N,N′*-Bis(2,6-dimethyl-4-fluorophenyl)ethylenediimine (3.24 g; 10.8 mmol, 1 equiv); $LiAlH_4$ (820 mg, 21.6 mmol, 2 equiv). *Workup A:* Yield: 3.33 g (82%). ^{1}H NMR (300 MHz, [D$_6$]DMSO): δ = 2.45 (s, 12H, $ArCH_3$), 3.53 (s, 4H, NCH_2CH_2N), 7.00 ppm (d, $^3J_{H,F}$ = 9 Hz, 4H, arom.); ^{13}C NMR (75 MHz,[D$_6$]DMSO): δ = 18.3, 46.6, 115.7 (d, $^2J_{C,F}$ = 23 Hz), 133.6, 134.5 (d, $^3J_{C,F}$ = 17 Hz), 159.8 ppm (d, $^1J_{C,F}$ = 243 Hz).

***N,N′*-Bis(2,6-dimethyl-4-chlorophenyl)ethylenediamine dihydrochloride (2g)**: *N,N′*-Bis(2,6-dimethyl-4-chlorophenyl)ethylenediimine (4.20 g, 12.6 mmol, 1 equiv); $LiAlH_4$ (547 mg, 14.4 mmol, 2 equiv). *Workup A*: Yield: 3.98 (77%). ^{1}H NMR (300 MHz, [D$_6$]DMSO): δ = 2.19 (s, 12H, $ArCH_3$), 3.26 (s, 4H, NCH_2CH_2N), 6.96 (s, 4H, arom.), 6.9–7.5 ppm (brs, 4H, NH_2); ^{13}C NMR (75 MHz, [D$_6$]DMSO): δ = 18.5, 47.0, 129.1, 130.2, 134.0, 137.6 ppm.

***N,N′*-Bis(2,6-dimethyl-4-iodophenyl)ethylenediamine dihydrochloride (2i)**: *N,N′*-Bis(2,6-dimethyl-4-iodophenyl)ethylenediimine (2.04 g, 3.95 mmol, 1 equiv); $LiAlH_4$ (300 mg, 7.9 mmol; 1 equiv). *Workup A*: Yield: 2.34 g (99%). ^{1}H NMR (300 MHz, [D$_6$]DMSO): δ = 2.31 (s, 12H, $ArCH_3$), 3.41 (s, 4H, NCH_2CH_2N), 6.4–7.3 (brs, 4H, NH_2), 7.36 ppm (s, 4H, arom.); ^{13}C NMR (75 MHz, [D$_6$]DMSO): δ = 17.8, 46.4, 91.1, 133.7, 137.2, 138.3 ppm.

***N*-(2-Iodoethyl)-2,6-dimethylaniline hydroiodide**: *N*-(2-Hydroxyethyl)-2,6-dimethylaniline hydroiodide (45.1 g, 273 mmol, 1 equiv) was placed in around bottom flask and cooled to 0°C. Aqueous HI (57%, 108 mL, 819 mmol, 3 equiv) was added dropwise with vigorous stirring. After the addition was completed the reaction mixture was heated to reflux for 24 h. After cooling to room temperature the product was filtered off and washed with Et_2O until the filtrate remained colorless. *N*-(2-Iodoethyl)-2,6-dimethylaniline hydroiodide was obtained as a yellow solid (90 g, 82%). ^{1}H NMR (300 MHz, [D$_6$]DMSO): δ = 2.41 (s, 6H, $ArCH_3$), 3.44 (t, 2H, NCH_2CH_2I), 3.44 (t, 2H, NCH_2CH_2I), 7.21 (s, 3H, arom.), 8.4 ppm (brs, 2H, NH_2); ^{13}C NMR (75 MHz, [D$_6$]DMSO): δ = −0.3, 18.7, 52.5, 128.5, 130.6, 132.3, 135.9 ppm.

***N*-(2-Hydroxyethyl)-2,6-dimethyl-4-bromoaniline**: 2,6-Dimethyl-4-bromoaniline (103 g, 515 mmol, 3 equiv) and 2-chloroethanol (11.5 mL, 172 mL, 1 equiv) were heated to 100°C for 48 h. The reaction mixture was poured into H_2O (300 mL), basified with solid KOH and extracted with CH_2Cl_2 (300 mL). The organic layer was dried over $MgSO_4$, the solvent was evaporated in vacuo and the residue distilled under reduced pressure (127°C, 0.2 mbar). Yield: 19.7 g (69%), viscous yellow oil. ^{1}H NMR (300 MHz, $CDCl_3$): δ = 2.0–3.0 (brs, 2H, NH + OH), 2.27 (s, 6H, $ArCH_3$), 3.10 (t, 2H, NCH_2CH_2OH), 3.75 (t, 2H, NCH_2CH_2I), 7.12 ppm (s, 2H, arom.); ^{13}C NMR (75 MHz, $CDCl_3$): δ = 18.3, 50.1, 62.1, 114.5, 131.3, 132.0, 144.7 ppm.

***N*-(2-Iodoethyl)-2,6-dimethyl-4-bromoaniline**: Ph_3P (32.7 g, 125 mmol, 2 equiv) was dissolved in CH_2CH_2 (400 mL). Imidazole (8.48 mg, 125 mmol, 2 equiv) and iodine (31.6 g, 125 mmol, 2 equiv) were added and the mixture was stirred for 30 min at room temperature. *N*-(2-Hydroxyethyl)-2,6-dimethyl-4-bromoaniline (15.2 g, 62.3 mmol, 1 equiv) dissolved in CH_2Cl_2 (100 mL) was added, the reaction mixture was stirred

for another 30 min and poured into H_2O (500 mL). The mixture was basified with solid $NaHCO_3$ and the organic layer was separated and dried over $MgSO_4$. The solvent was evaporated in vacuo and the residue was purified by column chromatography (silica, cyclohexane/ethyl acetate 10:1, $R_f = 0.36$) to yield the title compound as a brown oil (17.5 g, 80%). ^{1}H NMR (300 MHz, $CDCl_3$): $\delta = 2.27$ (s, 6H, $ArCH_3$), 3.25–3.30 (m, 4H, NCH_2CH_2I), 3.35 (br s, 1H, NH), 7.12 ppm (s, 2H, arom.); ^{13}C NMR (75 MHz, $CDCl_3$): $\delta = 6.9$, 18.6, 50.0, 114.8, 131.4, 131.8, 143.5 ppm.

General procedure for the synthesis of unsymmetrical diamines

N-(2-Iodoethyl)-2,6-dimethylaniline hydroiodide or *N*-(2-iodoethyl)-2,6-dimethyl-4-bromoaniline (1 equiv), the corresponding aniline (1 equiv) and $NaHCO_3$ (2–3 equiv) were dissolved in DMF (150 mL). The reaction mixture was stirred for 48 h at 50 °C, poured into an excess of water and extracted with Et_2O (3×200 mL). The combined organic layers were dried over $MgSO_4$ and the solvent was evaporated. The crude product was purified by column chromatography (silica gel, cyclohexane/ethyl acetate).

***N*-(2,6-Dimethylphenyl)-*N*′-(2,6-dimethyl-4-diethylaminophenyl)ethylenediamine (2m)**: *N*-(2-Iodoethyl)-2,6-dimethylaniline hydroiodide (12.09 g, 30 mmol, 1 equiv); 2,6-dimethyl-4-*N*,*N*′-diethylaminoaniline (5.77 g, 30 mmol, 1 equiv); $NaHCO_3$ (7.56 g, 90 mmol, 3 equiv). $R_f = 0.32$ (cyclohexane/ethyl acetate 4:1); yield: 5.29 g (52%), brown oil. ^{1}H NMR (300 MHz, [D$_6$]DMSO): $\delta = 1.13$ (t, 6H, CH_2CH_3), 2.29 (s, 6H, $ArCH_3$), 2.32 (s, 6H, $ArCH_3$), 3.08 (t, 2H, NCH_2CH_2N), 3.21 (t, 2H, NCH_2CH_2N), 3.28 (q, CH_2CH_3), 6.42 (s, 2H, arom.), 6.81 (t, $^3J_{H,H} = 7.5$ Hz, 1H, *p*-H), 6.99 ppm (d, $^3J_{H,H} = 7.5$ Hz, 2H, *m*-H); ^{13}C NMR (75 MHz, [D$_6$]DMSO): $\delta = 12.7$, 18.8, 49.0, 49.7, 113.3, 121.6, 128.9, 129.1, 132.2, 146.3 ppm.

***N*-(2,6-Dimethylphenyl)-*N*′-(2,6-dimethyl-4-bromophenyl)ethylenediamine (2n)**: *N*-(2-Iodoethyl)-2,6-dimethylaniline hydroiodide (4.00 g, 10 mmol, 1 equiv); 2,6-dimethyl-4-bromoaniline (2.00 g, 10 mmol, 1 equiv); $NaHCO_3$ (2.52 g, 30 mmol, 3 equiv). $R_f = 0.50$ (cyclohexane/ethyl acetate 4:1); yield: 1.40 g (68%), yellow solid. ^{1}H NMR (300 MHz, [D$_6$]DMSO): $\delta = 2.30$ (s, 6H, $ArCH_3$), 2.34 (s, 6H, $ArCH_3$), 3.23 (m, 4H, NCH_2CH_2N), 3.38 (s, 2H, NH), 6.88 (t, $^3J_{H,H} = 7.5$ Hz, 1H, *p*-H), 7.04 (d, $^3J_{H,H} = 7.5$ Hz, 2H, *m*-H), 7.16 ppm (s, 2H, arom.); ^{13}C NMR (75 MHz, [D$_6$]DMSO): $\delta = 18.6$, 18.7, 48.8, 49.0, 114.4, 122.2, 122.4, 129.0, 129.6, 131.5, 145.3, 145.9 ppm.

***N*-(2,6-Dimethyl-4-bromophenyl)-*N*′-(2,6-dimethyl-4-diethylaminophenyl)-ethylenediamine (2o)**: *N*-(2-Iodoethyl)-2,6-dimethyl-4-bromoaniline (6.00 g, 17.0 mmol, 1 equiv); 2,6-dimethyl-4-diethylaminoaniline (3.26 g, 17.0 mmol, 1 equiv); $NaHCO_3$ (2.85 g, 33.9 mmol, 2 equiv). $R_f = 0.23$ (cyclohexane/ethyl acetate 4:1); yield: 4.27 g (60%), brown oil. ^{1}H NMR (300 MHz, $CDCl_3$): $\delta = 1.26$ (t, 6H, CH_2CH_3), 2.40 (s, 6H, $ArCH_3$), 2.43 (s, 6H, $ArCH_3$), 3.17–3.20 (m, 2H, NCH_2CH_2N), 3.27–3.31 (m, 2H, NCH_2CH_2N), ≈3.4 (s, 2H, NH), 3.41 (q, 6H, CH_2CH_3), 6.55 (s, 2H, arom.), 7.23 ppm (s, 2H, arom.); ^{13}C NMR (75 MHz, $CDCl_3$): $\delta = 11.7$, 17.5, 17.8, 43.5, 47.9, 48.5, 112.2, 112.7, 130.1, 130.2, 131.2, 134.0. 143.1, 144.4 ppm.

General procedure for the synthesis of imidazolium chlorides 3·HCl

The corresponding diimine (1 equiv) was dissolved in anhydrous THF (10 mL per mmol) under an atmosphere of Ar. A solution of paraformaldehyde (1.25 equiv) in HCl in dioxane (4 M; 1.5 equiv) was prepared and added to the diimine solution at 0 °C via syringe. The reaction mixture was stirred at room temperature for 4 h, the white precipitate was filtered off, washed with Et_2O and dried in vacuo.

***N*,*N*′-Bis(2,6-dimethyl-4-methyloxyphenyl)imidazolium chloride (3b·HCl)**: *N*,*N*′-Bis(2,6-dimethyl-4-methoxyphenyl)ethylenediimine (234 mg, 0.72 mmol, 1 equiv), paraformaldehyde (27 mg, 0.90 mmol, 1.25 equiv); HCl in dioxane (4 M, 0.27 mL, 1.08 mmol, 1.5 equiv). Yield: 199 mg (74%). ^{1}H NMR (300 MHz, [D$_6$]DMSO): $\delta = 2.13$ (s, 12H, $ArCH_3$), 3.81 (s, 6H, OMe), 6.96 (s, 4H, arom.), 8.26 (s, 2H, NCHCHN), 9.71 ppm (s, 1H, imidazolium H); ^{13}C NMR (75 MHz, [D$_6$]DMSO): $\delta =$ 17.2, 55.6, 113.9, 125.0, 126.3, 136.1, 139.0, 160.2 ppm.

***N*,*N*′-Bis(2,6-dimethyl-4-thiomethylphenyl)imidazolium chloride (3e·HCl)**: *N*,*N*′-Bis(2,6-dimethyl-4-thiomethylphenyl)ethylenediimine (460 mg, 1.29 mmol, 1 equiv), paraformaldehyde (48 mg, 1.61 mmol, 1.25 equiv); HCl in dioxane (4 M, 0.48 mL, 1.92 mmol, 1.5 equiv). Yield: 413 mg (79%). ^{1}H NMR (300 MHz, [D$_6$]DMSO): $\delta = 2.15$ (s, 12H, $ArCH_3$), 2.50 (s, 6H, SMe), 7.27 (s, 4H, arom.), 8.30 (s, 2H, NCHCHN), 9.78 ppm (s, imidazolium H); ^{13}C NMR (75 MHz, [D$_6$]DMSO): $\delta = 14.4$, 16.9, 125.2, 126.5, 130.1, 135.1, 138.8, 141.8 ppm.

***N*,*N*′-Bis(2,6-dimethyl-4-fluorophenyl)imidazolium chloride (3f·HCl)**: *N*,*N*′-Bis(2,6-dimethyl-4-fluorophenyl)ethylenediimine (355 mg, 1.18 mmol, 1 equiv), paraformaldehyde (44 mg, 1.48 mmol, 1.25 equiv); HCl in dioxane (4 M, 0.44 mL, 1.77 mmol, 1.5 equiv). Yield: 366 mg (89%). ^{1}H NMR (300 MHz, [D$_6$]DMSO): $\delta = 2.11$ (s, 12H, $ArCH_3$), 7.26 (d, $^3J_{H,F} = 9$ Hz), 8.28 (s, 2H, NCHCHN), 9.77 ppm (s, 1H, imidazolium H); ^{13}C NMR (75 MHz, [D$_6$]DMSO): $\delta = 17.1$, 115.4 (d, $^2J_{C,F} = 23$ Hz), 124.8, 129.7, 137.6 (d, $^3J_{C,F} = 10$ Hz), 139.1, 162.3 ppm (d, $^1J_{C,F} = 247$ Hz).

***N*,*N*′-Bis(2,6-dimethyl-4-chlorophenyl)imidazolium chloride (3g·HCl)**: *N*,*N*′-Bis(2,6-dimethyl-4-chlorophenyl)ethylenediimine (680 mg, 2.04 mmol, 1 equiv), paraformaldehyde (77 mg, 2.55 mmol, 1.25 equiv); HCl in dioxane (4 M, 0.77 mL, 3.08 mmol, 1.5 equiv). Yield: 360 mg (46%). ^{1}H NMR (300 MHz, [D$_6$]DMSO): $\delta = 2.18$ (s, 12H, $ArCH_3$), 7.56 (s, 4H, arom), 8.35 (s, 2H, NCHCHN), 9.84 ppm (s, 1H, imidazolium H); ^{13}C NMR (75 MHz, [D$_6$]DMSO): $\delta = 15.9$, 123.8, 127.5, 131.3, 134.1, 136.3, 137.9 ppm.

***N*,*N*′-Bis(2,6-dimethyl-4-iodophenyl)imidazolium chloride (3i·HCl)**: *N*,*N*′-Bis(2,6-dimethyl-4-iodophenyl)ethylenediimine (1.00 g, 1.94 mmol, 1 equiv), paraformaldehyde (73 mg, 2.42 mmol, 1.25 equiv); HCl in dioxane (4 M, 0.73 mL, 2.91 mmol, 1.5 equiv). Yield: 912 mg (83%). ^{1}H NMR (300 MHz, [D$_6$]DMSO): $\delta = 2.12$ (s, 12H, $ArCH_3$), 7.82 (s, 4H, arom), 8.33 (s, 2H, NCHCHN), 9.86 ppm (s, 1H, imidazolium H); ^{13}C NMR (75 MHz, [D$_6$]DMSO): $\delta = 16.5$, 97.9, 124.6, 133.2, 137.0, 137.3, 138.5 ppm.

General procedure for the synthesis of imidazolinium chlorides 4·HCl

A) The corresponding diamine dihydrochloride was suspended in HC(OEt)$_3$ (5 mL per mmol), three drops of formic acid were added and the reaction mixture stirred at 120 °C over night. The white precipitate was filtered off, washed several times with Et_2O and dried in vacuo.

B) The corresponding diamine (1 equiv) and NH_4Cl (1 equiv) were suspended in HC(OEt)$_3$ and three drops of formic acid were added. The reaction mixture was stirred at 120 °C over night and poured into an excess of water. The aqueous phase was washed with Et_2O (2×100 mL) and extracted with CH_2Cl_2 (3×100 mL). The combined organic layers were dried over $MgSO_4$ and the solvent was evaporated in vacuo.

***N*,*N*′-Bis(2,6-dimethyl-4-methyloxyphenyl)imidazolinium chloride (4b·HCl)**: *Procedure A*: *N*,*N*′-Bis(2,6-dimethyl-4-methoxyphenyl)ethylenediamine dihydrochloride (310 mg, 0.77 mmol). Yield: 228 mg (79%). ^{1}H NMR (300 MHz, [D$_6$]DMSO): $\delta = 2.35$ (s, 12H, $ArCH_3$), 3.74 (s, 6H, OMe), 4.41 (s, NCH_2CH_2N), 6.84 (s, 4H, arom), 9.01 ppm (s, 1H, imidazolinium H); ^{13}C NMR (75 MHz, [D$_6$]DMSO): $\delta = 17.5$, 51.0, 55.4, 113.9, 126.2, 137.2, 159.6, 160.7 ppm.

***N*,*N*′-Bis(2,6-dimethyl-4-thiomethylphenyl)imidazolinium chloride (4e·HCl)**: *Procedure A*: *N*,*N*′-Bis(2,6-dimethyl-4-thiomethylphenyl)ethylenediamine dihydrochloride (944 mg, 2.18 mmol). Yield: 607 mg (69%). ^{1}H NMR (300 MHz, [D$_6$]DMSO): $\delta = 2.41$ (s, 12H, $ArCH_3$), 2.50 (s, 6H, SMe), 4.45 (s, 4H, NCH_2CH_2N), 7.15 (s, 4H, arom), 9.12 ppm (s, 1H, imidazolinium H); ^{13}C NMR (75 MHz, [D$_6$]DMSO): $\delta = 14.4$, 17.3, 50.9, 125.4, 130.1, 136.3, 140.6, 160.4 ppm.

***N*,*N*′-Bis(2,6-dimethyl-4-fluorophenyl)imidazolinium chloride (4f·HCl)**: *Procedure A*: *N*,*N*′-Bis(2,6-dimethyl-4-fluorophenyl)ethylenediamine dihydrochloride (1.13 g, 2.99 mmol, 1 equiv). Yield: 880 mg (84%). ^{1}H NMR (500 MHz, [D$_6$]DMSO): $\delta = 2.30$ (s, 12H, $ArCH_3$), 4.40 (s, 4H, NCH_2CH_2N), 7.10 (d, $^3J_{H,F=}9$ Hz), 9.02 ppm (s, 1H, imidazolinium H); ^{13}C NMR (126 MHz, [D$_6$]DMSO): $\delta = 17.8$, 51.3, 115.8 (d, $^2J_{C,F} = 22$ Hz), 130.1 (d, $^4J_{C,F} = 2$ Hz), 139.3 ($^3J_{C,F} = 11$ Hz), 161.2, 162.2 ppm (d, $^1J_{C,F} =$ 247 Hz).

***N*,*N*′-Bis(2,6-dimethyl-4-chlorophenyl)imidazolinium chloride (4g·HCl)**: *Procedure A*: *N*,*N*′-Bis(2,6-dimethyl-4-chlorophenyl)ethylenediamine dihydrochloride (2.26 mg, 5.51 mmol, 1 equiv). Yield: 1.51 mg (71%). ^{1}H NMR (500 MHz, [D$_6$]DMSO): $\delta = 2.28$ (s, 12H, $ArCH_3$), 4.37 (s, 4H, NCH_2CH_2N), 7.29 (s, 4H, arom.), 9.08 ppm (s, 1H, imidazolinium H);

^{13}C NMR (126 MHz, [D$_6$]DMSO): δ = 17.6, 51.2, 128.9, 132.7, 134.5, 138.7, 160.9 ppm.

***N,N′*-Bis(2,6-dimethyl-4-iodophenyl)imidazolinium chloride (4i·HCl)**: *Procedure A:* *N,N′*-Bis(2,6-dimethyl-4-iodophenyl)ethylenediamine dihydrochloride (1.30 g, 2.19 mmol, 1 equiv). Yield: 944 mg (76%). ^{1}H NMR (300 MHz, [D$_6$]DMSO): δ = 2.34 (s, 12H, ArCH$_3$), 4.45 (s, 4H, NCH$_2$CH$_2$N), 7.69 (s, 4H, arom.), 9.08 ppm (s, 1H, imidazolinium H); ^{13}C NMR (75 MHz, [D$_6$]DMSO): δ = 16.8, 50.7, 96.9, 133.3, 137.3, 138.3, 160.2 ppm.

***N*-(2,6-Dimethylphenyl)-*N′*-(2,6-dimethyl-4-diethylaminophenyl)imidazolinium chloride (4m)**: *Procedure B:* *N*-(2,6-Dimethylphenyl)-*N′*-(2,6-dimethyl-4-*N,N′*-diethylaminophenyl)ethylenediamine (4.35 g, 12.8 mmol, 1 equiv); NH_4Cl (685 mg, 12.8 mmol, 1 equiv); HC(OEt)$_3$ (21.3 mL, 128 mmol, 10 equiv). Yield: 3.52 g (71%). ^{1}H NMR (300 MHz, [D$_6$]DMSO): δ = 1.07 (t, 6H, CH$_2$CH$_3$), 2.30 (s, 6H, ArCH$_3$), 2.38 (s, 6H, ArCH$_3$), 3.34 (q, 4H, CH$_2$CH$_3$), 4.43 (m, 4H, NCH$_2$CH$_2$N), 6.47 (s, 2H, arom.), 7.26 (m, 2H, *m*-H), 7.35 (m, 1H, *p*-H), 9.02 ppm (s, 1H, imidazolinium H); ^{13}C NMR (75 MHz, [D$_6$]DMSO): δ = 12.4, 17.3, 17.8, 43.6, 50.7, 51.4, 110.7, 121.0, 128.9, 129.9, 133.5, 135.8, 136.0, 147.8, 160.4 ppm.

***N*-(2,6-Dimethylphenyl)-*N′*-(2,6-dimethyl-4-bromophenyl)imidazolinium chloride (4n)**: *Procedure B:* *N*-(2,6-Dimethylphenyl)-*N′*-(2,6-dimethyl-4-bromophenyl)ethylenediamine (2.26 g, 6.50 mmol, 1 equiv); NH_4Cl (348 mg, 6.50 mmol, 1 equiv); HC(OEt)$_3$ (10.8 mL, 65 mmol, 10 equiv). Yield: 2.00 g (79%). ^{1}H NMR (300 MHz, [D$_6$]DMSO): δ = 2.42 (s, 12H, ArCH$_3$), 4.51 (s, 4H, NCH$_2$CH$_2$N), 7.25–7.40 (m, 3H, arom.), 7.56 (s, 2H, arom.), 9.18 ppm (s, 1H, imidazolinium H); ^{13}C NMR (75 MHz, [D$_6$]DMSO): δ = 17.1, 17.3, 50.7, 50.9, 122.8, 128.9, 130.0, 131.4, 132.8, 133.3, 135.7, 138.6, 160.1 ppm.

***N*-(2,6-Dimethyl-4-diethylaminophenyl)-*N′*-(2,6-dimethyl-4-bromophenyl)-imidazolinium chloride (4o)**: *Procedure B:* *N*-(2,6-dimethyl-4-bromophenyl)-*N′*-(2,6-dimethyl-4-diethylaminophenyl)ethylenediamine (4.29 g, 10.3 mmol, 1 equiv); NH_4Cl (548 mg, 10.3 mmol, 1 equiv); HC(OEt)$_3$ (17.1 mL, 103 mmol, 10 equiv). Yield: 1.21 g (25%). ^{1}H NMR (300 MHz, [D$_6$]DMSO): δ = 1.07 (t, 6H, CH$_2$CH$_3$), 2.29 (s, 6H, ArCH$_3$), 2.38 (s, 6H, ArCH$_3$), 3.34 (q, 4H, CH$_2$CH$_3$), 4.41 (m, 4H, NCH$_2$CH$_2$N), 6.46 (s, 2H, arom.), 7.53 (s, 2H, arom.), 9.02 ppm (s, 1H, imidazolinium H); ^{13}C NMR (75 MHz, [D$_6$]DMSO): δ = 12.4, 17.1, 17.8, 43.6, 50.6, 51.5, 110.7, 120.9, 122.7, 131.4, 133.0, 136.0, 138.6, 147.9, 160.5 ppm.

General Procedure for the synthesis of Grubbs II complexes 5 and 6

The corresponding azolium salt (1.5 or 2 equiv) and KO*t*Bu (1.5 or 2 equiv) were weighed in a Schlenk tube under an atmosphere of argon. Toluene was added and the mixture was stirred for 30 min. Dichlorobenzylidenebis(tricyclohexylphosphine)ruthenium (1 equiv) was added as a solid under a stream of argon. The mixture was stirred for 1 h at 50°C. The solvent was evaporated in vacuo and the crude product was purified by column chromatography (silica gel, cyclohexane/ethyl acetate 10:1).

Cl$_2$Ru=CHPh(3a)PCy$_3$ (5a): *N,N′*-Bis(2,6-dimethyl-4-*N,N′*-diethylaminophenyl)imidazolium chloride (341 mg, 0.75 mmol, 1.5 equiv), KO*t*Bu (84 mg, 0.75 mmol, 1.5 equiv), dichlorobenzylidenebis(tricyclohexylphosphine)ruthenium (412 mg, 0.5 mmol, 1 equiv). R_f = 0.22; yield: 384 mg (82%); brown solid. ^{1}H NMR (CDCl$_3$, 500 MHz): δ = 19.42 (s, 1H, RuCH), 9.0 (brs, 1H, *o*-H benzylidene), 7.33 (t, *J* = 7.0 Hz, 1H, *p*-H benzylidene), 7.08 (brs, 3H, *o*- + *m*-H benzylidene), 6.96 (s, 1H, NCHCHN), 6.93 (s, 1H, NCHCHN), 6.46 (s, 2H, *m*-H aryl$_{NHC}$), 6.2 (brs, 1H, *m*-H aryl$_{NHC}$), 5.4 (brs, 1H, *m*-H aryl$_{NHC}$), 3.39 (q, 4H, CH$_2$CH$_3$), 3.15 (q, 4H, CH$_2$CH$_3$), 2.45 (brs, 6H, ArCH$_3$), 2.27 (m, 3H, PCH), 2.0 (brs, 6H, ArCH$_3$), 1.4–1.6 (m, 15H, Cy), 1.23 (t, 6H, CH$_2$CH$_3$), 1.13 (t, 6H, CH$_2$CH$_3$), 0.9–1.1 ppm (m, 15H, Cy); ^{13}C NMR (CDCl$_3$, 126 MHz): δ = 293.6, 189.2 (d, $J_{C,P}$ = 84 Hz), 151.0. 147.0, 146.5, 138.1, 136.2, 127.1, 126.6, 125.4, 124.1, 123.6, 109.2, 108.4, 43.0, 42.9, 30.5 (d, $J_{P,C}$ = 16 Hz), 28.3, 26.9, 26.8, 25.4, 19.3, 11.9, 11.8 ppm; ^{31}P NMR (CDCl$_3$, 202 MHz): δ = 31.0 ppm.

Cl$_2$Ru=CHPh(3b)PCy$_3$ (5b): *N,N′*-Bis(2,6-dimethyl-4-methoxyphenyl)-imidazolium chloride (150 mg, 0.40 mmol, 1.5 equiv), KO*t*Bu (45 mg, 0.40 mmol, 1.5 equiv), dichlorobenzylidenebis(tricyclohexylphosphine)ruthenium (220 mg, 0.27 mmol, 1 equiv). Yield: 210 mg (90%); red solid. ^{1}H NMR (CDCl$_3$, 500 MHz): δ = 19.38 (s, 1H, RuCH), 9.0 (brs, 1H, *o*-H benzylidene), 7.33 (t, *J* = 7.5 Hz, 1H, *p*-H benzylidene), 7.07 (t, *J* = 7.5 Hz, 2H, *m*-H benzylidene), 7.0 (brs, 1H, *o*-H benzylidene), 6.92 (s, 2H, NCHCHN), 6.68 (s, 2H, *m*-H aryl$_{NHC}$), 6.4 (brs, 1H, *m*-H aryl$_{NHC}$), 5.5 (brs, 1H, *m*-H aryl$_{NHC}$), 3.76 (s, 3H, OMe), 3.48, (s, 3H, OMe), 2.4 (brs, 6H, ArCH$_3$), 2.11 (q, 3H, PCH), 1.8 (brs, 6H, ArCH$_3$), 1.44 (m, 8H, Cy), 1.32 (m, 7H, Cy), 0.8–1.0 ppm (m, 15H, Cy); ^{13}C NMR (CDCl$_3$, 126 MHz): δ = 293.9, 189.2 (d, $J_{C,P}$ = 83 Hz), 158.6, 158.0, 150.8, 138.8, 131.3, 129.8, 126.9, 123.8, 123.5, 112.5, 54.1, 53.6, 30.7 (d, $J_{C,P}$ = 17 Hz), 28.2, 26.8, 26.7, 26.0, 25.9, 25.4, 25.2, 19.0, 17.7 ppm; ^{31}P NMR (CDCl$_3$, 202 MHz): δ = 31.5 ppm.

Cl$_2$Ru=CHPh(3d)PCy$_3$ (5d): *N,N′*-Bis(2,6-dimethylphenyl)imidazolium chloride (313 mg, 1.00 mmol, 1.5 equiv), KO*t*Bu (112 mg, 1.00 mmol, 1.5 equiv), dichlorobenzylidenebis(tricyclohexylphosphine)ruthenium (550 mg, 0.67 mmol, 1 equiv). R_f = 0.20; yield: 405 mg (74%); red solid. ^{1}H NMR (CDCl$_3$, 500 MHz): δ = 19.9 (s, 1H, RuCH), 8.3 (brs, 1H, *o*-H benzylidene), 7.15 (t, *J* = 7.0 Hz, 1H, *p*-H benzylidene), 7.11 (s, 2H, aryl$_{NHC}$), 7.07 (brs, 3H, NCHCHN + *o*-H benzylidene), 6.97 (t, *J* = 7.5 Hz, 2H, *m*-H benzylidene), 6.54 (t, *J* = 7.5 Hz, 1H, *p*-H aryl$_{NHC}$), 6.4 (brs, 1H, aryl$_{NHC}$), 6.09 (s, 2H, aryl$_{NHC}$), 2.61 (s, 6H, ArCH$_3$), 2.45 (m, 3H, PCH), 2.21 (brs, 6H, ArCH$_3$), 1.4–1.7 (m, 15H, Cy), 1.0–1.2 ppm (m, 15H, Cy); ^{13}C NMR (CDCl$_3$, 126 MHz): δ = 294.5, 188.7 (d, $J_{C,P}$ = 83 Hz), 151.2, 138.2, 137.6, 137.0, 135.5, 131.3, 128.7, 127.9, 127.4, 123.0, 122.6, 30.9 (d, $J_{C,P}$ = 16 Hz), 28.3, 26.9 (d, $J_{C,P}$ = 10 Hz), 26.3, 25.9, 25.3, 18.9, 17.5 ppm; ^{31}P NMR (CDCl$_3$, 202 MHz): δ = 31.4 ppm.

Cl$_2$Ru=CHPh(3e)PCy$_3$ (5e): *N,N′*-Bis(2,6-dimethyl-4-thiomethylphenyl)-imidazolium chloride (178 mg, 0.44 mmol, 1.5 equiv), KO*t*Bu (49 mg, 0.44 mmol, 1.5 equiv), dichlorobenzylidenebis(tricyclohexylphosphine)ruthenium (241 mg, 0.29 mmol, 1 equiv). R_f = 0.24; yield: 210 mg (80%); red solid. ^{1}H NMR (CDCl$_3$, 500 MHz): δ = 19.43 (s, 1H, RuCH), 9.0 (brs, 1H, *o*-H benzylidene), 7.41 (t, *J* = 7.3 Hz, 1H, *p*-H benzylidene), 7.2 (brs, 1H, *o*-H benzylidene), 7.16 (t, *J* = 7.3 Hz, 2H, *m*-H benzylidene), 7.05 (s, 2H, *m*-H aryl$_{NHC}$), 6.96 (s, 1H, NCHCHN), 6.95 (s, 1H, NCHCHN), 6.9 (brs, 1H, *m*-H aryl$_{NHC}$), 5.9 (brs, 1H, *m*-H aryl$_{NHC}$), 2.50 (s, 3H, SCH$_3$), 2.5 (brs, 6H, ArCH$_3$), 2.28 (s, 3H, SCH$_3$), 2.2 (brs, 3H, ArCH$_3$), 2.23 (m, 3H, PCH), 2.0 (brs, 3H, ArCH$_3$), 1.53 (brs, 9H, Cy), 1.42 (brs, 6H, Cy), 0.9–1.1 ppm (brs, 15H, Cy); ^{13}C NMR (CDCl$_3$, 126 MHz): δ = 295.5, 190.0 (d, $J_{C,P}$ = 82 Hz), 151.9, 140.3, 139.3, 138.9, 137.1, 136.2, 134.8, 128.2, 125.4, 124.9, 124.7, 124.5, 31.8 (d, $J_{C,P}$ = 16 Hz), 26.4, 27.9 (d, $J_{C,P}$ = 10 Hz), 27.0, 26.5, 19.9, 18.7, 15.0, 14.8 ppm; ^{31}P NMR (CDCl$_3$, 202 MHz): δ = 31.7 ppm.

Cl$_2$Ru=CHPh(3f)PCy$_3$ (5f): *N,N′*-Bis(2,6-dimethyl-4-fluorophenyl)imidazolium chloride (148 mg, 0.42 mmol, 1.5 equiv), KO*t*Bu (48 mg, 0.42 mmol, 1.5 equiv), dichlorobenzylidenebis(tricyclohexylphosphine)ruthenium (233 mg, 0.28 mmol, 1 equiv). R_f = 0.21; yield: 216 mg (90%); pink solid. ^{1}H NMR (CDCl$_3$, 500 MHz): δ = 19.46 (s, 1H, RuCH), 9.0 (brs, 1H, *o*-H benzylidene), 7.43 (t, *J* = 6.8 Hz, 1H, *p*-H benzylidene), 7.2 (brs, 1H, *o*-H benzylidene), 7.16 (t, *J* = Hz, 2H, *m*-H benzylidene), 7.00 (s, 1H, NCHCHN), 6.96 (s, 1H, NCHCHN), 6.94 (d, *J*(H,F) = 8.5 Hz, 2H, *m*-H aryl$_{NHC}$), 6.6 (brs, 1H, *m*-H aryl$_{NHC}$), 5.8 (brs, 1H, *m*-H aryl$_{NHC}$), 2.48 (brs, 6H, ArCH$_3$), 2.22 (q, 3H, PCH), 1.8–2.4 (brs, 6H, ArCH$_3$), 1.53 (brs, 9H, Cy), 1.42 (brs, 6H, Cy), 1.03 (brs, 9H, Cy), 0.95 ppm (brs, 6H, Cy); ^{13}C NMR (CDCl$_3$, 126 MHz): δ = 294.1, 189.5 (d, $J_{C,P}$ = 81 Hz), 162.2 (d, $J_{C,F}$ = 67 Hz), 160.3 (d, $J_{C,F}$ = 67 Hz), 150.6, 140.1, 138.0, 133.9, 132.6, 127.5, 127.2, 123.8, 123.5, 114.2 (d, $J_{C,F}$ = 21 Hz), 113.5 (d, $J_{C,F}$ = 23 Hz), 30.8 (d, $J_{C,P}$ = 18 Hz), 28.2, 26.8 (d, $J_{C,P}$ = 10 Hz), 25.2, 19.0, 17.7 ppm; ^{31}P NMR (CDCl$_3$, 202 MHz): δ = 31.6 ppm.

Cl$_2$Ru=CHPh(3g)PCy$_3$ (5g): *N,N′*-Bis(2,6-dimethyl-4-chlorophenyl)imidazolium chloride (586 mg, 1.54 mmol, 1.5 equiv), KO*t*Bu (172 mg, 1.54 mmol, 1.5 equiv), dichlorobenzylidenebis(tricyclohexylphosphine)ruthenium (632 mg, 0.77 mmol, 1 equiv). R_f = 0.41; yield: 651 mg (95%); pink solid. ^{1}H NMR (CDCl$_3$, 500 MHz): δ = 19.45 (s, 1H, RuCH), 8.9 (brs, 1H, *o*-H benzylidene), 7.47 (t, *J* = 7.0 Hz, 1H, *p*-H benzylidene), 7.24 (s, 2H, *m*-H aryl$_{NHC}$), 7.20 (m, 3H, *m*-H benzylidene + *o*-H benzylidene), 7.00 (s, 1H, NCHCHN), 6.97 (s, 1H, NCHCHN), 7.0 (brs, 1H, *m*-H aryl$_{NHC}$), 6.1 (brs, 1H, *m*-H aryl$_{NHC}$), 2.47 (s, 6H ArCH$_3$), 2.23 (q, 3H, PCH), 2.2 (brs, 3H, ArCH$_3$), 1.9 (brs, 3H, ArCH$_3$), 1.56 (brs, 9H, Cy), 1.43 (brs, 6H, Cy), 0.8–1.1 ppm (m, 15H, Cy); ^{13}C NMR (CDCl$_3$, 126 MHz): δ = 294.3, 189.3 (d, $J_{C,P}$ = 82 Hz), 150.5, 139.3, 136.5, 135.5,

135.2, 134.3, 133.4, 127.7, 127.6, 127.3, 126.9, 123.7, 123.3, 30.8 (d, $J_{C,P}$ = 17 Hz), 28.3, 26.8, 26.7, 25.3, 18.7, 17.5 ppm; ^{31}P NMR ($CDCl_3$, 202 MHz): δ = 32.0 ppm.

Cl_2Ru=CHPh(3h)PCy_3 (5h): *N,N′*-Bis(2,6-dimethyl-4-bromophenyl)imidazolium chloride (214 mg, 0.45 mmol, 1.5 equiv), KO*t*Bu (51 mg, 0.45 mmol, 1.5 equiv), dichlorobenzylidenebis(tricyclohexylphosphine)ruthenium (249 mg, 0.30 mmol, 1 equiv). R_f = 0.38; yield: 274 mg (92%); pink solid. ^{1}H NMR ($CDCl_3$, 500 MHz): δ = 19.45 (s, 1H, RuCH), 8.9 (brs, 1H, *o*-H benzylidene), 7.48 (t, J = 7.3 Hz, 1H, *p*-H, benzylidene), 7.40 (s, 2H, *m*-H aryl$_{NHC}$), 7.22 (m, 3H, *m*-H benzylidene + *o*-H benzylidene), 7.2 (brs, 1H, *m*-H aryl$_{NHC}$), 6.99 (s, 1H, NCHCHN), 6.96 (s, 1H, NCHCHN), 6.2 (brs, 1H, *m*-H aryl$_{NHC}$), 2.47 (brs, 6H, $ArCH_3$), 2.23 (q, 3H, PCH), 1.7–2.1 (brs, 6H, $ArCH_3$), 1.57 (brs, 9H, Cy), 1.43 (brs, 6H, Cy), 0.8–1.1 ppm (m, 15H, Cy); ^{13}C NMR ($CDCl_3$, 126 MHz): δ = 294.4, 189.3 (d, $J_{C,P}$ = 82 Hz), 150.5, 139.6, 137.7, 137.0, 135.8, 130.6, 129.8, 127.6, 127.4, 123.7, 123.3, 122.9, 122.0, 30.8 (d, $J_{C,P}$ = 17.6 Hz), 28.3, 26.8, 26.7, 25.3, 18.6, 17.4 ppm; ^{31}P NMR ($CDCl_3$, 202 MHz): δ = 32.0 ppm.

Cl_2Ru=CHPh(3i)PCy_3 (5i): *N,N′*-Bis(2,6-dimethyl-4-iodophenyl)imidazolium chloride (210 mg, 0.37 mmol, 1.5 equiv), KO*t*Bu (42 mg, 0.37 mmol, 1.5 equiv), dichlorobenzylidenebis(tricyclohexylphosphine)ruthenium (204 mg, 0.25 mmol, 1 equiv). Yield: 200 mg (75%); pink solid. ^{1}H NMR ($CDCl_3$, 500 MHz): δ = 19.43 (s, 1H, RuCH), 8.9 (brs, 1H, *o*-H benzylidene), 7.60 (s, 2H, *m*-H aryl$_{NHC}$), 7.50 (t, 1H, *p*-H benzylidene), 7.25 (brs, 4H, *o*-H benzylidene + *m*-H benzylidene + *m*-H aryl$_{NHC}$), 6.98 (m, 1H, NCHCHN), 6.95 (m, 1H, NCHCHN), 6.5 (brs, 1H, *m*-H aryl$_{NHC}$), 2.5 (brs, 9H $ArCH_3$), 2.23 (q, 3H, PCH), 2.0 (brs, 3H, $ArCH_3$), 1.57 (brs, 9H, Cy), 1.42 (brs, 6H, Cy), 0.9–1.1 ppm (m, 15H, Cy); ^{13}C NMR ($CDCl_3$, 126 MHz): δ = 294.4, 189.1 (d, $J_{C,P}$ = 82 Hz), 150.5, 139.6, 137.8, 136.6, 135.8, 127.6, 127.5, 123.6, 123.2, 95.6, 94.9, 30.7 (d, $J_{P,C}$ = 17.6 Hz), 28.3, 26.8, 26.7, 26.3, 26.1, 26.0, 25.9, 18.3, 17.2 ppm; ^{31}P NMR ($CDCl_3$, 202 MHz): δ = 31.9 ppm.

Cl_2Ru=CHPh(4a)PCy_3 (6a): *N,N′*-Bis(2,6-dimethyl-4-N,N′-diethylaminophenyl)imidazolinium chloride (808 mg, 1.77 mmol, 2 equiv), KO*t*Bu (199 mg, 1.77 mmol, 2 equiv), dichlorobenzylidenebis(tricyclohexylphosphine)ruthenium (727 mg, 0.88 mmol, 1 equiv). R_f = 0.29; yield: 660 mg (78%); brown solid. ^{1}H NMR ($CDCl_3$, 500 MHz): δ = 19.14 (s, 1H, RuCH), 9.1 (brs, 1H, *o*-H benzylidene), 7.30 (t, J = 7.5 Hz, 1H, *p*-H benzylidene), 7.1 (m, 3H, *o*- + *m*-H benzylidene), 6.45 (s, 2H, *m*-H aryl$_{NHC}$), 6.2 (brs, 1H, *m*-H aryl$_{NHC}$), 5.3 (brs, 1H, *m*-H aryl$_{NHC}$), 3.9 (brs, 4H, NCH_2CH_2N), 3.37 (q, 4H, CH_2CH_3), 3.12 (brs, 4H, CH_2CH_3), 2.4–2.7 (brs, 9H, $ArCH_3$), 2.23 (m, 3H, PCH), 2.0 (brs, 3H, $ArCH_3$), 1.3–1.6 (m, 15H, Cy), 1.22 (t, 6H, CH_2CH_3), 1.11 (t, 6H, CH_2CH_3), 0.9–1.1 ppm (m, 15H, Cy); ^{13}C NMR ($CDCl_3$, 126 MHz): δ = 292.7, 219.9 (d, $J_{C,P}$ = 78 Hz), 150.7. 146.6, 146.0, 139.1, 137.0, 127.4, 126.6, 215.0, 109.8, 108.8, 51.7, 50.6, 42.9, 42.8, 30.4 (d, $J_{C,P}$ = 16 Hz), 28.1, 26.8, 26.7, 25.9, 25.6, 25.4, 21.3, 19.7, 18.3, 11.9 ppm; ^{31}P NMR ($CDCl_3$, 202 MHz): δ = 29.3 ppm.

Cl_2Ru=CHPh(4b)PCy_3 (6b): *N,N′*-Bis(2,6-dimethyl-4-methoxyphenyl)-imidazolinium chloride (150 mg, 0.40 mmol, 2 equiv), KO*t*Bu (45 mg, 0.40 mmol, 2 equiv), dichlorobenzylidenebis(tricyclohexylphosphine)ruthenium (165 mg, 0.20 mmol, 1 equiv). Yield: 99 mg (56%); red solid. ^{1}H NMR ($CDCl_3$, 500 MHz): δ = 19.15 (s, 1H, RuCH), 9.0 (brs, 1H, *o*-H benzylidene), 7.35 (t, J = 8.0 Hz, 1H, *p*-H benzylidene), 7.1 (brs, 3H, *m*-H benzylidene + *o*-H benzylidene), 6.71 (s, 2H, *m*-H aryl$_{NHC}$), 6.5 (brs, 1H, *m*-H aryl$_{NHC}$), 5.5 (brs, 1H, *m*-H aryl$_{NHC}$), 3.9–4.0 (brs, 4H, NCH_2CH_2N), 3.80 (s, 3H, OMe), 3.51, (s, 3H, OMe), 2.4–2.8 (brs, 9H, $ArCH_3$), 2.19 (q, 3H, PCH), 2.1 (brs, 3H, $ArCH_3$), 1.3–1.6 (m, 15H, Cy), 0.8–1.0 ppm (m, 15H, Cy); ^{13}C NMR ($CDCl_3$, 126 MHz): δ = 293.1, 220.0 (d, $J_{C,P}$ = 77 Hz), 158.0. 157.4, 139.7, 137.4, 131.7, 131.2, 129.6, 128.6, 127.0, 125.1, 112.8, 111.2, 54.0, 53.6, 51.3, 50.4, 30.5 (d, $J_{C,P}$ = 16 Hz), 28.1, 26.8, 26.7, 25.2, 19.5, 18.0 ppm; ^{31}P NMR ($CDCl_3$, 202 MHz): δ = 29.3 ppm.

Cl_2Ru=CHPh(4d)PCy_3 (6d): *N,N′*-Bis(2,6-dimethylphenyl)imidazolinium chloride (157 mg, 0.5 mmol, 2 equiv), KO*t*Bu (56 mg, 0.5 mmol, 2 equiv), dichlorobenzylidenebis(tricyclohexylphosphine)ruthenium (205 mg, 0.25 mmol, 1 equiv). R_f = 0.31; yield: 105 mg (51%); red solid. ^{1}H NMR ($CDCl_3$, 500 MHz): δ = 19.16 (s, 1H, RuCH), 9.0 (brs, 1H, *o*-H benzylidene), 7.33 (t, J = 7.0 Hz, 1H, *p*-H benzylidene), 7.22 (m, 3H, *m*-H benzylidene + aryl$_{NHC}$), 7.08 (s, 3H, aryl$_{NHC}$), 7.0 (brs, 1H, *o*-H benzylidene), 6.58 (t, J = 7.5 Hz, 1H, *p*-H aryl$_{NHC}$), 6.1 (brs, 1H, *m*-H aryl$_{NHC}$), 4.04 (m, 2H, NCH_2CH_2N), 3.90 (brs, 2H, NCH_2CH_2N), 2.7 (brs, 9H, $ArCH_3$), 2.2 (brs, 3H, $ArCH_3$), 2.16 (q, 3H, PCH), 1.49 (m, 9H, Cy), 1.34 (m, 6H, Cy), 1.01, (m, 9H, Cy), 0.7–0.9 ppm (m, 6H, Cy); ^{13}C NMR ($CDCl_3$, 126 MHz): δ = 293.9, 219.1 (d, $J_{C,P}$ = 77 Hz), 150.4, 138.3, 136.5, 136.2, 128.1, 127.9, 127.3, 127.1, 126.7, 51.0, 50.3, 30.5 (d, $J_{C,P}$ = 18 Hz), 30.5, 28.9, 28.0, 26.7, 25.4, 25.1, 19.6, 17.8 ppm; ^{31}P NMR ($CDCl_3$, 202 MHz): δ = 29.0 ppm.

Cl_2Ru=CHPh(4e)PCy_3 (6e): *N,N′*-Bis(2,6-dimethyl-4-thiomethylphenyl)-imidazolinium chloride (163 mg, 0.40 mmol, 2 equiv), KO*t*Bu (45 mg, 0.40 mmol, 2 equiv), dichlorobenzylidenebis(tricyclohexylphosphine)ruthenium (165 mg, 0.20 mmol, 1 equiv). Yield: 111 mg (61%); red solid. ^{1}H NMR ($CDCl_3$, 500 MHz): δ = 19.08 (s, 1H, RuCH), 8.94 (brs, 1H, *o*-H benzylidene), 7.31 (t, J = 7.0 Hz, 1H, *p*-H benzylidene), 7.09 (t, J = 7.0 Hz, 2H, *m*-H benzylidene), 7.0 (brs, 1H, *o*-H benzylidene), 6.96 (s, 2H, *m*-aryl$_{NHC}$), 6.75 (brs, 1H, *m*-aryl$_{NHC}$), 5.75 (s, 1H, *m*-aryl$_{NHC}$), 3.7–3.9 (m, 4H, NCHCHN), 2.56 (brs, 3H, $ArCH_3$), 2.51 (brs, 3H, $ArCH_3$), 2.41 (s, 3H, SMe), 2.18 (s, 3H, SMe), 2.12 (m, 3H, PCH), 2.11 (brs, 3H, $ArCH_3$), 1.3–1.5 (m, 15H, Cy), 0.8–0.9 ppm (m, 15H, Cy); ^{13}C NMR ($CDCl_3$, 126 MHz): δ = 150.3, 138.2, 137.2, 135.6, 133.5, 127.1, 124.8, 124.0, 54.7, 51.2, 30.5 (d, $J_{C,P}$ = 17.6 Hz), 28.0, 26.8, 26.7, 25.3, 19.1, 17.8, 14.0, 13.7 ppm; Ru*C*H and RuC_{NHC} were not observed; ^{31}P NMR ($CDCl_3$, 202 MHz): δ = 29.6 ppm.

Cl_2Ru=CHPh(4f)PCy_3 (6f): *N,N′*-Bis(2,6-dimethyl-4-fluorophenyl)imidazolinium chloride (256 mg, 0.73 mmol, 2 equiv), KO*t*Bu (82 mg, 0.73 mmol, 2 equiv), dichlorobenzylidenebis(tricyclohexylphosphine)ruthenium (300 mg, 0.365 mmol, 1 equiv). R_f = 0.21; yield: 187 mg (60%); pink solid. ^{1}H NMR ($CDCl_3$, 500 MHz): δ = 19.17 (s, 1H, RuCH), 9.00 (brs, 1H, *o*-H benzylidene), 7.40 (t, J = 7.5 Hz, 1H, *p*-H benzylidene), 7.14 (*t*, J = 7.5 Hz, 2H, *m*-H benzylidene), 7.05 (brs, 1H, *o*-H benzlidene), 6.89 (d, J(H,F) = 8.5 Hz, 2H, *m*-H aryl$_{NHC}$), 6.63 (brs, 1H, *m*-H aryl$_{NHC}$), 5.67 (brs, 1H, *m*-H aryl$_{NHC}$), 3.8–4.1 (m, 4H, NCH_2CH_2N), 2.4–2.8 (m, 9H, $ArCH_3$), 2.18 (q, 3H, PCH), 2.06 (brs, 3H, $ArCH_3$), 1.5 (brs, 9H, Cy), 1.4 (brs, 6H, Cy), 1.0 (brs, 9H, Cy), 0.9 ppm (brs, 6H, Cy); ^{13}C NMR ($CDCl_3$, 126 MHz): δ = 293.5, 220.6 (d, $J_{C,P}$ = 77 Hz), 161.8 (d, $J_{C,F}$ = 79 Hz), 159.8 (d, $J_{C,F}$ = 79 Hz), 150.2, 140.9, 138.5, 133.4 (d, $J_{C,F}$ = 250 Hz), 127.6, 127.1, 114.5 (d, $J_{C,F}$ = 22 Hz), 113.7 (d, $J_{C,F}$ = 22 Hz), 51.1, 50.3, 30.6 (d, $J_{C,P}$ = 17 Hz), 28.1, 26.7 (d, $J_{C,P}$ = 12 Hz), 25.1, 19.4, 17.9 ppm; ^{31}P NMR ($CDCl_3$, 202 MHz): δ = 29.3 ppm.

Cl_2Ru=CHPh(4g)PCy_3 (6g): *N,N′*-Bis(2,6-dimethyl-4-chlorophenyl)imidazolinium chloride (384 mg, 1.00 mmol, 2 equiv), KO*t*Bu (112 mg, 1.00 mmol, 2 equiv), dichlorobenzylidenebis(tricyclohexylphosphine)ruthenium (412 mg, 0.50 mmol, 1 equiv). R_f = 0.25; yield: 307 mg (69%); pink solid. ^{1}H NMR ($CDCl_3$, 500 MHz): δ = 19.08 (s, 1H, RuCH), 8.90 (brs, 1H, *o*-H benzylidene), 7.37 (t, J = 7.5 Hz, 1H, *p*-H benzylidene), 7.11 (m, 4H, *m*-H benzylidene + *m*-H aryl$_{NHC}$), 6.9 (m, 2H, *o*-H benzylidene + *m*-H aryl$_{NHC}$), 5.89 (brs, 1H, *m*-H aryl$_{NHC}$), 3.7–3.9 (m, 4H, NCH_2CH_2N), 2.52 (brs, 3H, $ArCH_3$), 2.47 (brs, 6H, $ArCH_3$), 2.12 (q, 3H, PCH), 2.0 (brs, 3H, $ArCH_3$), 1.2–1.4 (m, 15H, Cy), 0.8–0.9 ppm (m, 15H, Cy); ^{13}C NMR ($CDCl_3$, 126 MHz): δ = 293.6, 220.4 (d, $J_{C,P}$ = 77 Hz), 150.0, 140.1, 138.1, 136.9, 135.0, 133.5, 132.5, 130.8, 128.7, 128.0, 127.6, 127.1, 51.0, 50.9, 30.5 (d, $J_{C,P}$ = 16.3 Hz), 28.2, 28.0, 26.7, 26.6, 25.9, 25.3, 25.2, 19.1, 17.6 ppm; ^{31}P NMR ($CDCl_3$, 202 MHz): δ = 29.8 ppm.

Cl_2Ru=CHPh(4h)PCy_3 (6h): *N,N′*-Bis(2,6-dimethyl-4-bromophenyl)imidazolinium chloride (149 mg, 0.32 mmol, 2 equiv), KO*t*Bu (35 mg, 0.32 mmol, 2 equiv), dichlorobenzylidenebis(tricyclohexylphosphine)ruthenium (130 mg, 0.16 mmol, 1 equiv). R_f = 0.20; yield: 126 mg (81%); pink solid. ^{1}H NMR ($CDCl_3$, 500 MHz): δ = 19.14 (s, 1H, RuCH), 8.97 (s, 1H, *o*-H benzylidene), 7.44 (t, J = 7.8 Hz, 1H, *p*-H benzylidene), 7.35 (s, 2H, *m*-H aryl$_{NHC}$), 7.0–7.2 (brs, 4H, *o*-H benzylidene + *m*-H benzylidene + *m*-H aryl$_{NHC}$), 6.13 (brs, 1H, *m*-H aryl$_{NHC}$), 3.7–4.1 (m, 4H, NCH_2CH_2N), 2.78 (brs, 3H $ArCH_3$), 2.5–2.6 (m, 6H, $ArCH_3$), 2.19 (q, 3H, PCH), 2.03 (brs, 3H, $ArCH_3$), 1.2–1.6 (m, 15H, Cy), 0.8–1.1 ppm (m, 15H, Cy); ^{13}C NMR ($CDCl_3$, 126 MHz): δ = 293.7, 220.4 (d, $J_{C,P}$ = 77 Hz), 150.1, 137.5, 135.6, 131.0, 130.2, 127.7, 127.3, 122.1, 121.2, 50.9, 50.2, 30.6 (d, $J_{C,P}$ = 17 Hz), 28.3, 26.8 (d, $J_{C,P}$ = 10 Hz), 25.3, 19.0, 17.7 ppm; ^{31}P NMR ($CDCl_3$, 202 MHz): δ = 30.0 ppm.

$Cl_2Ru{=}CHPh(4i)PCy_3$ (6i): *N*,*N*′-Bis(2,6-dimethyl-4-iodophenyl)imidazolinium chloride (296 mg, 0.52 mmol, 2 equiv), KO*t*Bu (59 mg, 0.52 mmol, 2 equiv), dichlorobenzylidenebis(tricyclohexylphosphine)ruthenium (215 mg, 0.26 mmol, 1 equiv). R_f=0.23; yield: 137 mg (49%); pink solid. ^{1}H NMR ($CDCl_3$, 500 MHz): δ=19.14 (s, 1H, RuCH), 8.96 (brs, 1H, *o*-H benzylidene), 7.55 (s, 2H, *m*-H aryl$_{NHC}$), 7.46 (t, J=7.3 Hz, 1H, *p*-H benzylidene), 7.1–7.4 (m, 3H, *m*-H benzylidene + *o*-H benzylidene), 7.01 (brs, 1H, *m*-H aryl$_{NHC}$), 6.35 (brs, 1H, *m*-H aryl$_{NHC}$), 3.7–4.1 (brs, 4H, NCH_2CH_2N), 2.74 (brs, 3H, $ArCH_3$), 2.4–2.6 (m, 6H, $ArCH_3$), 2.19 (m, 3H, PCH), 2.01 (brs, 3H, $ArCH_3$), 1.2–1.6 (m, 15H, Cy), 0.8–1.1 ppm (m, 15H, Cy); ^{13}C NMR ($CDCl_3$, 126 MHz): δ=294.8, 221.3 (d, $J_{C,P}$=77 Hz), 151.1, 141.8, 139.6, 139.4, 138.1, 137.5, 137.1, 128.7, 128.5, 96.0, 95.2, 31.7 (d, $J_{C,P}$=17 Hz), 29.4, 29.1, 27.8 (d, $J_{C,P}$=8 Hz), 26.5, 19.9, 18.6 ppm; ^{31}P NMR ($CDCl_3$, 202 MHz): δ=29.9 ppm.

$Cl_2Ru{=}CHPh(4m)PCy_3$ (6m): *N*-(2,6-Dimethylphenyl)-*N*′-(2,6-dimethyl-4-diethylaminophenyl)imidazolinium chloride (386 mg, 1.00 mmol, 2 equiv), KO*t*Bu (112 mg, 1.00 mmol, 2 equiv), dichlorobenzylidenebis-(tricyclohexylphosphine)ruthenium (412 mg, 0.50 mmol, 1 equiv). R_f= 0.29; yield: 421 mg (94%); brown solid. ^{1}H NMR ($CDCl_3$, 500 MHz): δ= (mixture of 2 isomers) 19.19 (s, RuCH, minor isomer), 19.11 (s, RuCH, major isomer), 9.00 (brs, *o*-H benzylidene), 7.27–7.33 (m, *p*-H benzylidene + *p*-H aryl$_{NHC(H)}$), 7.18–7.23 (m, *m*-H benzylidene), 7.06 (brs, *o*-H benzylidene + *m*-H aryl$_{NHC(H)}$), ca. 6.9 (brs, *m*-H aryl$_{NHC}$), 6.55 (t, J= 7.3 Hz, *p*-H aryl$_{NHC}$), 6.44 (s, *m*-H aryl$_{NHC(NEt_2)}$), ca. 6.2 (brs, *m*-H aryl$_{NHC}$), 5.33 (brs, *m*-H aryl$_{NHC}$), 3.7–4.1 (m, NCH_2CH_2N), 3.36 (q, CH_2CH_3), 3.11 (q, CH_2CH_3), 2.65 (brs, $ArCH_3$), ca. 2.5 (brs, $ArCH_3$), 2.18 (m, PCH), ca 2.1 (brs, $ArCH_3$), 1.49 (brs, Cy), 1.37 (brs, Cy), 1.20 (t, CH_2CH_3), 1.09 (t, CH_2CH_3), 0.8–1.1 ppm (m, Cy); ^{13}C NMR ($CDCl_3$, 126 MHz): δ=220.2 (d, $J_{C,P}$=79 Hz), 218.9 (d, $J_{C,P}$=79 Hz), 150.6, 146.7, 146.2, 138.6, 136.8, 128.0, 127.9, 127.2, 127.2, 126.9, 126.9, 126.7, 109.9, 51.8, 50.9, 50.8, 50.2, 42.9, 42.8, 30.6 (d, $J_{C,P}$=16 Hz), 30.5 (d, $J_{C,P}$=16 Hz), 28.1, 28.8, 28.7, 25.4, 24.2, 19.7, 19.1, 18.3, 13.1, 11.9 ppm; ^{31}P NMR ($CDCl_3$, 202 MHz): δ=28.5 (minor isomer), 27.8 ppm (major isomer).

$Cl_2Ru{=}CHPh(4n)PCy_3$ (6n): *N*-(2,6-Dimethylphenyl)-*N*′-(2,6-dimethyl-4-bromophenyl)imidazolinium chloride (310 mg, 0.787 mmol, 2 equiv), KO*t*Bu (88 mg, 0.787 mmol, 2 equiv), dichlorobenzylidenebis(tricyclohexylphosphine)ruthenium (324 mg, 0.394 mmol, 1 equiv). R_f=0.29; yield: 255 mg (72%); pink solid. ^{1}H NMR ($CDCl_3$, 500 MHz): δ=(mixture of 2 isomers) 19.20 (s, RuCH, major isomer), 19.12 (s, RuCH, minor isomer), 9.01 (brs, *o*-H benzylidene), 7.44 (t, J=7.5 Hz, *p*-H benzylidene), 7.35 (s, *m*-H aryl$_{NHC(Br)}$, minor isomer), 7.33 (t, J=7.5 Hz, *m*-H benzylidene), 7.15–7.25 (m, orho H benzylidene + *m*-H aryl$_{NHC}$, minor isomer), 7.08 (brs, *m*-H aryl$_{NHC}$), 6.58 (t, 8.2 Hz, *p*-H aryl$_{NHC}$, major isomer), 6.13 (brs, *m*-H aryl$_{NHC}$), 3.7–4.1 (m, NCH_2CH_2N), 2.5–2.9 (m, $ArCH_3$), 2.18 (q, 3H, PCH), 2.06 (brs, 3H, $ArCH_3$), 1.2–1.6 (brs, Cy), 0.7–1.1 ppm (brs, Cy); ^{13}C NMR ($CDCl_3$, 126 MHz): δ=293.4, 219.7 (d, $J_{C,P}$=77 Hz), 150.3, 150.1, 138.2, 137.6, 136.3, 130.9, 130.1, 128.3, 128.0, 127.5, 127.4, 127.3, 127.2, 122.0, 121.1, 51.0, 50.3, 50.1, 30.6 (d, $J_{C,P}$=17 Hz), 30.5 (d, $J_{C,P}$= 17 Hz), 28.1, 26.8, 26.7, 19.1, 19.1, 17.8 ppm; ^{31}P NMR ($CDCl_3$, 202 MHz): δ=29.6 (major isomer), 29.2 ppm (minor isomer).

$Cl_2Ru{=}CHPh(4o)PCy_3$ (6o): *N*-(2,6-Dimethyl-4-bromophenyl)-*N*′-(2,6-dimethyl-4-diethylaminophenyl)imidazolinium chloride (218 mg, 0.47 mmol, 2 equiv), KO*t*Bu (53 mg, 0.47 mmol, 2 equiv), dichlorobenzylidenebis(tricyclohexylphosphine)ruthenium (193 mg, 0.23 mmol, 1 equiv). R_f=0.30; yield: 163 mg (72%); brown solid. ^{1}H NMR ($CDCl_3$, 500 MHz): δ=(mixture of 2 isomers) 19.14 (s, RuCH, major isomer), 18.98 (s, RuCH, minor isomer), 9.01 (brs, *o*-H benzylidene), 7.43 (t, J= 7.5 Hz, *p*-H benzylidene), 7.34 (s, arom., minor isomer), 7.19 (t, J= 7.5 Hz, *m*-H benzylidene), 7.07 (brs, orho H benzylidene + *m*-H aryl$_{NHC}$), 6.43 (s, *m*-H aryl$_{NHC(NEt2)}$, major isomer), 6.58 (t, 8.2 Hz, *p*-H aryl$_{NHC}$, major isomer), 6.13 (brs, *m*-H aryl$_{NHC}$), 3.7–4.1 (m, NCH_2CH_2N), 3.35 (q, CH_2CH_3), 3.11 (q, CH_2CH_3), 2.4–2.8 (m, $ArCH_3$), 2.1–2.3 (m, PCH), 2.06 (brs, $ArCH_3$), 1.3–1.6 (brs, Cy), 1.20 (t, CH_2CH_3), 1.09 (t, CH_2CH_3), 0.88 (t, CH_2CH_3), 0.8–1.1 ppm (brs, Cy); ^{13}C NMR ($CDCl_3$, 126 MHz): δ=292.6, 220.6 (d, $J_{C,P}$=77 Hz), 219.4 (d, $J_{C,P}$=77 Hz),150.5, 150.3, 146.8, 146.2, 137.9, 136.1, 130.9, 130.4, 127.3, 127.2, 127.0, 124.5, 121.8, 120.9, 109.9, 51.9, 50.8, 50.0, 42.9, 42.8, 30.5 (d, $J_{C,P}$=15 Hz), 30.2 (d, $J_{C,P}$=11 Hz), 28.2, 26.8, 26.7, 26.0, 25.6, 25.4, 25.3, 19.7, 19.1, 11.9 ppm; ^{31}P NMR ($CDCl_3$, 202 MHz): δ=29.8 (major isomer), 28.6 ppm (minor isomer).

Oxidation and reduction of 6m: Compound **6m** (140 mg, 0.171 mmol, 1 equiv) and ferrocenium tetrafluoroborate (47 mg, 0.171 mmol, 1 equiv) were placed in a Schlenk tube and dissolved in dry and degassed CH_2Cl_2 (5 mL). The solution was stirred for 1 h at room temperature and the volatiles were removed in vacuo. The residue was suspended in toluene (5 mL), vigorously stirred for 30 min and filtered off. The orange-brown solid was washed with pentane until the washings remained colorless and dried in vacuo. Yield: 124 mg (80%). Some of this material (35 mg, 0.039 mmol, 1 quiv) was placed in a Schlenk tube, dissolved in dry and degassed CH_2Cl_2 (3.5 mL) and cooled to −78°C. Octamethylferrocene (12 mg, 0.039 mmol, 1 quiv) was added and the mixture was stirred for 30 min at −78°C. During that time, a color change from dark red to a dark green-blue occurred. The reaction mixture was poured onto a column (silica gel) and eluted with Et_2O (50 mL precooled to −30°C). The volatiles were removed in vacuo at −78°C and the residue was dissolved in CD_2Cl_2 (0.8 mL, precooled to −78°C) for NMR analysis. The filtrate is free from paramagnetic impurities.

CCDC 665252 contains the supplementary crystallographic data for this paper. These data can be obtained free of charge from The Cambridge Crystallographic Data Centre via www.ccdc.cam.ac.uk/data_request/cif.

Acknowledgements

This work was supported by the Deutsche Forschungsgemeinschaft and the Fonds der Chemischen Industrie. We wish to thank Ms. I. Svoboda for the crystal structure analysis and Prof. Dr. R. Schäfer for helpful discussions. C.M.T. thanks Professor M. Reggelin for helpful discussions and for his support.

[1] *N-Heterocyclic Carbenes in Transition Metal Catalysis* (Ed.: F. Glorius), Springer, Berlin, **2007**.
[2] R. H. Grubbs, *Tetrahedron* **2004**, *60*, 7117–7140.
[3] K. Vehlow, S. Maechling, S. Blechert, *Organometallics* **2006**, *25*, 25–28.
[4] G. Occhipinti, H.-R. Bjørsvik, V. R. Jensen, *J. Am. Chem. Soc.* **2006**, *128*, 6952–6964.
[5] Ł. Gułajski, A. Michrowskaa, R. Bujok, K. Grela, *J. Mol. Catal. A* **2006**, *254*, 118–123.
[6] E. Colacino, J. Martinez, F. Lamaty, *Coord. Chem. Rev.* **2007**, *251*, 726–764.
[7] P. H. Deshmukh, S. Blechert, *Dalton Trans.* **2007**, 2479–2491.
[8] O. Navarro, N. Marion, J. Mei, S. P. Nolan, *Chem. Eur. J.* **2006**, *12*, 5142–5148.
[9] N. Marion, O. Navarro, J. Mei, E. D. Stevens, N. M. Scott, S. P. Nolan, *J. Am. Chem. Soc.* **2006**, *128*, 4101–4111.
[10] C. W. K. Gstöttmayr, V. P. W. Böhm, E. Herdtweck, M. Grosche, W. A. Herrmann, *Angew. Chem.* **2002**, *114*, 1421–1423; *Angew. Chem. Int. Ed.* **2002**, *41*, 1363–1365.
[11] G. Altenhoff, R. Goddard, C. W. Lehmann, F. Glorius, *J. Am. Chem. Soc.* **2004**, *126*, 15195–15201.
[12] E. A. B. Kantchev, C. J. O'Brien, M. G. Organ, *Angew. Chem.* **2007**, *119*, 2824–2870; *Angew. Chem. Int. Ed.* **2007**, *46*, 2768–2813.
[13] C. A. Fleckenstein, S. Roy, S. Leuthäußer, H. Plenio, *Chem. Commun.* **2007**, 2870–2872.
[14] S. Diez-Gonzalez, S. P. Nolan, *Coord. Chem. Rev.* **2007**, *251*, 874–883.
[15] F. E. Hahn, *Angew. Chem.* **2006**, *118*, 1374–1378; *Angew. Chem. Int. Ed.* **2006**, *45*, 1348–1352.
[16] S. Leuthäußer, D. Schwarz, H. Plenio, *Chem. Eur. J.* **2007**, *13*, 7195–7203.
[17] A. R. Chianese, A. Kovacevic, B. M. Zeglis, J. W. Faller, R. H. Crabtree, *Organometallics* **2004**, *23*, 2461–2468.

[18] A. R. Chianese, X. Li, M. C. Janzen, J. W. Faller, R. H. Crabtree, *Organometallics* **2003**, *22*, 1663–1667.
[19] S. Gómez-Bujedo, M. Alcarazo, C. Pichon, E. Álvarez, R. Fernández, J. M. Lassaletta, *Chem. Commun.* **2007**, 1180–1182.
[20] M. Viciano, E. Mas-Marzá, M. Sanaú, E. Peris, *Organometallics* **2006**, *25*, 3063–3069.
[21] F. C. Courchay, J. C. Sworen, A. Coronado, K. B. Wagener, *J. Mol. Catal. A* **2006**, *254*, 111–117.
[22] N. Hadei, E. A. B. Kantchev, C. J. O'Brien, M. G. Organ, *Org. Lett.* **2005**, *7*, 1991–1994.
[23] W. W. Schoeller, D. Schroeder, A. B. Rozhenko, *J. Organomet. Chem.* **2005**, *690*, 6079–6088.
[24] C. Präsang, B. Donnadieu, G. Bertrand, *J. Am. Chem. Soc.* **2005**, *127*, 10182–10183.
[25] J. C. Green, B. J. Herbert, *Dalton Trans.* **2005**, 1214–1220.
[26] A. M. Magill, K. J. Cavell, B. F. Yates, *J. Am. Chem. Soc.* **2004**, *126*, 8717–8724.
[27] S. Saravanakumar, A. I. Oprea, M. Kindermann, P. G. Jones, J. Heinicke, *Chem. Eur. J.* **2006**, *12*, 3143–3154.
[28] F. E. Hahn, M. C. Jahnke, T. Pape, *Organometallics* **2007**, *26*, 150–154.
[29] R. Dorta, E. D. Stevens, N. M. Scott, C. Costabile, L. Cavallo, C. D. Hoff, S. P. Nolan, *J. Am. Chem. Soc.* **2005**, *127*, 2485–2495.
[30] W. A. Herrmann, J. Schütz, G. D. Frey, E. Herdtweck, *Organometallics* **2006**, *25*, 2437–2448.
[31] N. M. Scott, R. Dorta, E. D. Stevens, A. Correa, L. Cavallo, S. P. Nolan, *J. Am. Chem. Soc.* **2005**, *127*, 3516–3526.
[32] X. Hu, I. Castro-Rodriguez, K. Olsen, K. Meyer, *Organometallics* **2004**, *23*, 755–764.
[33] M. D. Sanderson, J. W. Kamplain, C. W. Bielawski, *J. Am. Chem. Soc.* **2007**, *129*, 16514–16515.
[34] D. Nemcsok, K. Wichmann, G. Frenking, *Organometallics* **2004**, *23*, 3640–3646.
[35] L. Mercs, G. Labat, A. Neels, A. Ehlers, M. Albrecht, *Organometallics* **2006**, *25*, 5648–5656.
[36] H. Jacobsen, A. Correa, C. Costabile, L. Cavallo, *J. Organomet. Chem.* **2006**, *691*, 4350–4358.
[37] D. M. Khramov, V. M. Lynch, C. W. Bielawski, *Organometallics* **2007**, *26*, 6042–6049.
[38] A. Fürstner, L. Ackermann, B. Gabor, R. Goddard, C. W. Lehmann, R. Mynott, F. Stelzer, O. R. Thiel, *Chem. Eur. J.* **2001**, *7*, 3236–3253.
[39] J. A. Love, M. S. Sanford, M. W. Day, R. H. Grubbs, *J. Am. Chem. Soc.* **2003**, *125*, 10103–10109.
[40] N. Ledoux, B. Allaert, A. Linden, P. V. D. Voort, F. Verpoort, *Organometallics* **2007**, *26*, 1052–1056.
[41] T. Ritter, M. W. Day, R. H. Grubbs, *J. Am. Chem. Soc.* **2006**, *128*, 11768–11769.
[42] M. B. Dinger, P. Nieczypor, J. C. Mol, *Organometallics* **2003**, *22*, 5291–5296.
[43] M. Süßner, H. Plenio, *Chem. Commun.* **2005**, 5417–5419.
[44] L. Delaude, S. Delfosse, A. Richel, A. Demonceau, A. F. Noels, *Chem. Commun.* **2003**, 1526–1527.
[45] A. Richel, A. Demonceau, A. F. Noels, *Tetrahedron Lett.* **2006**, *47*, 2077–2081.
[46] C. Janiak, *J. Chem. Soc. Dalton Trans.* **2000**, 3885–3896.
[47] N. Ledoux, B. Allaert, S. Pattyn, H. V. Mierde, C. Vercaemst, F. Verpoort, *Chem. Eur. J.* **2006**, *12*, 4654–4661.
[48] M. Barbasiewicz, M. Bieniek, A. Michrowska, A. Szadkowska, A. Makal, K. Wozniak, K. Grela, *Adv. Synth. Catal.* **2007**, *349*, 193–203.
[49] D. R. Anderson, V. Lavallo, D. J. O'Leary, G. Bertrand, R. H. Grubbs, *Angew. Chem.* **2007**, *119*, 7400–7403; *Angew. Chem. Int. Ed.* **2007**, *46*, 7262–7265.
[50] K. Vehlow, S. Gessler, S. Blechert, *Angew. Chem.* **2007**, *119*, 8228–8231; *Angew. Chem. Int. Ed.* **2007**, *46*, 8082–8085.
[51] G. C. Vougioukalakis, R. H. Grubbs, *Organometallics* **2007**, *26*, 2469–2472.
[52] G. Xu, S. R. Gilbertson, *Org. Lett.* **2005**, *7*, 4605–4608.
[53] A. W. Waltman, R. H. Grubbs, *Organometallics* **2004**, *23*, 3105–3107.
[54] A. W. Waltman, T. Ritter, R. H. Grubbs, *Organometallics* **2006**, *25*, 4238–4239.
[55] A. Paczal, A. C. Bényei, A. Kotschy, *J. Org. Chem.* **2006**, *71*, 5969–5979.
[56] A. Fürstner, M. Alcarazo, V. César, C. W. Lehmann, *Chem. Commun.* **2006**, 2176–2178.
[57] F. E. Hahn, M. Paas, D. L. Van, R. Fröhlich, *Chem. Eur. J.* **2005**, *11*, 5080–5085.
[58] B. Rhodes, J. C. W. Chien, J. S. Wood, A. Chandrasekaran, M. D. Rausch, *J. Organomet. Chem.* **2001**, *625*, 95–100.
[59] T. M. Trnka, J. P. Morgan, M. S. Sanford, T. E. Wilhelm, M. Scholl, T.-L. Choi, S. Ding, M. W. Day, R. H. Grubbs, *J. Am. Chem. Soc.* **2003**, *125*, 2546–2558.
[60] T. Ritter, A. Hejl, A. G. Wenzel, T. W. Funk, R. H. Grubbs, *Organometallics* **2006**, *25*, 5740–5745.
[61] Phosphines, which are larger and more electron donating, and likewise halogens, which are smaller and more electron withdrawing, lead to more active catalysts.
[62] E. L. Dias, S. T. Nguyen, R. H. Grubbs, *J. Am. Chem. Soc.* **1997**, *119*, 3887–3897.
[63] C. W. Bielawski, R. H. Grubbs, *Angew. Chem.* **2000**, *112*, 3025–3028; *Angew. Chem. Int. Ed.* **2000**, *39*, 2903–2905.
[64] M. Süßner, H. Plenio, *Angew. Chem.* **2005**, *117*, 7045–7048; *Angew. Chem. Int. Ed.* **2005**, *44*, 6885–6888.
[65] C. Hansch, A. Leo, R. W. Taft, *Chem. Rev.* **1991**, *91*, 165–195.
[66] K. Getty, M. U. Delgado-Jaime, P. Kennepohl, *J. Am. Chem. Soc.* **2007**, *129*, 15774–15776.
[67] H. Plenio, C. Aberle, *Chem. Eur. J.* **2001**, *7*, 4438–4446.
[68] H. Plenio, C. Aberle, Y. A. Shihadeh, J. M. Lloris, R. Martinez-Manez, T. Pardo, J. Soto, *Chem. Eur. J.* **2001**, *7*, 2848–2861.
[69] H. Plenio, C. Aberle, *Angew. Chem.* **1998**, *110*, 1467–1470; *Angew. Chem. Int. Ed.* **1998**, *37*, 1397–1399.
[70] H. Plenio, J. Yang, R. Diodone, J. Heinze, *Inorg. Chem.* **1994**, *33*, 4098–4104.
[71] R. Gleiter, R. Roers, J. Classen, A. Jacobi, G. Huttner, T. Oeser, *Organometallics* **2000**, *19*, 147–151.
[72] M. E. Stoll, S. R. Lovelace, W. E. Geiger, H. Schimanke, I. Hyla-Kryspin, R. Gleiter, *J. Am. Chem. Soc.* **1999**, *121*, 9343–9351.
[73] R. J. Schaller, G. Haberhauer, R. Gleiter, F. Rominger, *Eur. J. Inorg. Chem.* **2002**, 2296–2304.
[74] R. H. Voegeli, H. C. Kang, R. G. Finke, V. Boekelheide, *J. Am. Chem. Soc.* **1986**, *108*, 7010–7016.
[75] B. Gollas, B. Speiser, I. Zagos, C. Maichle-Mössmer, *J. Organomet. Chem.* **2000**, *602*, 75–90.
[76] B. Speiser, "Molecular electrochemistry of cyclophanes" in *Modern Cyclophane Chemistry* (Eds.: R. Gleiter, H. Hopf), Wiley-VCH, Weinheim, **2004**.
[77] A. C. Hillier, W. J. Sommer, B. S. Yong, J. L. Petersen, L. Cavallo, S. P. Nolan, *Organometallics* **2003**, *22*, 4322–4326.
[78] H. Clavier, S. P. Nolan, *Chem. Eur. J.* **2007**, *13*, 8029–8036.
[79] J. Schleucher, J. Quant, S. J. Glaser, C. Griesinger, *J. Magn. Reson. Ser. A* **1995**, *112*, 144–151.
[80] H. Kessler, H. Oschkinat, C. Griesinger, W. Bermel, *J. Magn. Reson.* **1986**, *70*, 106–133.
[81] J. Stonehouse, P. Adell, J. Keeler, A. J. Shaka, *J. Am. Chem. Soc.* **1994**, *116*, 6037–6038.
[82] K. Stott, J. Stonehouse, J. Keeler, T. L. Hwang, A. J. Shaka, *J. Am. Chem. Soc.* **1995**, *117*, 4199–4200.
[83] S. Macura, B. T. Farmer, L. R. Brown, *J. Magn. Reson.* **1986**, *70*, 493–499.
[84] H. Hu, K. Krishnamurthy, *J. Magn. Reson.* **2006**, *182*, 173–177.
[85] Considerable decomposition takes place at temperatures above 60 °C, such that temperature dependent quantification of rotation rates could not be performed.
[86] N. G. Connelly, W. E. Geiger, *Chem. Rev.* **1996**, *96*, 877–910.
[87] C. D. Abernethy, G. M. Codd, M. D. Spicer, M. K. Taylor, *J. Am. Chem. Soc.* **2003**, *125*, 1128–1129.

[88] The ratio of the cathodic and anodic Ru^{III} isomers is governed by the difference of the respective redox potentials according to $\ln K = zF/RT \cdot \Delta E$. For $\Delta E = 219$ mV the cathodic isomer is formed in $> 99\,\%$ yield.
[89] C. L. Perrin, T. J. Dwyer, *Chem. Rev.* **1990**, *90*, 935–967.
[90] H. Kessler, *Angew. Chem.* **1970**, *82*, 237–253; *Angew. Chem. Int. Ed. Engl.* **1970**, *9*, 219–235.
[91] Z. L. Lu, A. Mayr, K. K. Cheung, *Inorg. Chim. Acta* **1999**, *284*, 205–214.
[92] G. Valkanas, *J. Chem. Soc. Dalton Trans.* **1963**, 5554–5556.
[93] P. F. Ranken, B. G. McKinnie, *J. Org. Chem.* **1989**, *54*, 2985–2988.
[94] L. Delaude, M. Szypa, A. Demonceau, A. F. Noels, *Adv. Synth. Catal.* **2002**, *344*, 749–756.
[95] Exchange-mediated ROE (or vice versa) can be excluded due to different temperature dependence (see Figure S4, Supporting Information).

Received: January 23, 2008
Published online: May 6, 2008

